Examensarbete
LITH-ITN-MT-EX--05/010--SE

Digital 3D Facial Reconstruction Based on Computed Tomography

Björn Andersson
Martin Valfridsson

2005-02-18

Linköpings universitet
TEKNISKA HÖGSKOLAN

Department of Science and Technology
Linköpings Universitet
SE-601 74 Norrköping, Sweden

Institutionen för teknik och naturvetenskap
Linköpings Universitet
601 74 Norrköping

LITH-ITN-MT-EX--05/010--SE

Digital 3D Facial Reconstruction Based on Computed Tomography

Examensarbete utfört i medieteknik
vid Linköpings Tekniska Högskola, Campus Norrköping

Björn Andersson
Martin Valfridsson

Handledare Michael Pääbo (PCG AB)
Handledare Gunilla Holmlund (RMV)
Handledare Calle Winskog (RMV)
Handledare Anders Persson (CMIV)
Examinator Björn Gudmundsson

Norrköping 2005-02-18

Avdelning, Institution
Division, Department

Institutionen för teknik och naturvetenskap

Department of Science and Technology

Datum
Date

2005-02-18

Språk
Language

☐ Svenska/Swedish
☒ Engelska/English

☐ _______________

Rapporttyp
Report category

Examensarbete
☐ B-uppsats
☐ C-uppsats
☒ D-uppsats

☐ _______________

ISBN

ISRN LITH-ITN-MT-EX--05/010--SE

Serietitel och serienummer
Title of series, numbering

ISSN

URL för elektronisk version
http://www.ep.liu.se/exjobb/itn/2005/mt/010/

Titel
Title

Digital 3D Facial Reconstruction Based on Computed Tomography

Författare
Author

Björn Andersson, Martin Valfridsson

Sammanfattning
Abstract

Despite the introduction of DNA-analysis for identification of human remains (1997-2000) several cases exist where the deceased remain unidentified. Approximately ten percent of unknown deceased persons can not be identified
by dental status or other present methods. During the year 2003 alone, seven individuals, in Sweden, remain unidentified.

Increase in travel in Europe will lead to more discoveries of foreign human remains in Sweden. In these cases, dental and medical records are often unavailable for the identification process.
When reconstructing a face from a skull, a technique with so called landmarks is used. These landmarks define the distance between the skull and the skin.

Today the reconstruction is performed by a forensic artist applying modelling clay to a cast of the skull according to the placement of the landmarks. This method is considered unethical since it involves manipulation of the skull. Another drawback with this method is that it is very time consuming and changes and modifications of the model are hard to do.

This thesis presents the possibilities of digitally, in 3D, reconstructing deceased
persons' faces based on computed tomography of skulls. This is done by presenting our PC based 3D modelling tool that we have implemented in
Discreet 3ds max. By developing and testing our software we have shown that digital 3D facial reconstruction can be performed by acquiring data from CT and performing the reconstruction process in 3ds max with help from our software.

Nyckelord
Keyword

3D, face, facial, reconstruction, CT, Computed Tomography, forensic, identification, 3ds max, modelling, facial approximation

Digital 3D Facial Reconstruction Based on Computed Tomography

February 22, 2005

Björn Andersson
Martin Valfridsson

Abstract

Despite the introduction of DNA-analysis for identification of human remains (1997-2000) several cases exist where the deceased remain unidentified. Approximately ten percent of unknown deceased persons can not be identified by dental status or other present methods. During the year 2003 alone, seven individuals, in Sweden, remain unidentified. Increase in travel in Europe will lead to more discoveries of foreign human remains in Sweden. In these cases, dental and medical records are often unavailable for the identification process.

When reconstructing a face from a skull, a technique with so called landmarks is used. These landmarks define the distance between the skull and the skin. Today the reconstruction is performed by a forensic artist applying modelling clay to a cast of the skull according to the placement of the landmarks. This method is considered unethical since it involves manipulation of the skull. Another drawback with this method is that it is very time consuming and changes and modifications of the model are hard to do.

This thesis presents the possibilities of digitally, in 3D, reconstructing deceased persons' faces based on computed tomography of skulls. This is done by presenting our PC based 3D modelling tool that we have implemented in Discreet 3ds max. By developing and testing our software we have shown that digital 3D facial reconstruction can be performed by acquiring data from CT and performing the reconstruction process in 3ds max with help from our software.

Preface

This Master thesis is based on the work conducted by us at Pääbo Consulting Group AB in Linköping from September 2004 to February 2005.

The work has been interesting since we have had to study both technical and medical literature and it has widened our understanding of the human body, work in the forensic field and programming.

We would like to thank the following persons for making this thesis possible.

- Michael and Eva Pääbo for inviting us into the friendly atmosphere at PCG and for continuous support during the project.
- Ulf Textorius for support on 3ds max and 3D modelling
- Calle Winskog, Gunilla Holmlund and Johan Berge of the National Board of Forensic Medicine (RMV) for providing expertise on forensic sciences and for presenting the different departments at RMV to us.
- The National Board of Forensic Medicine for economically and legally making the clinical tests possible.
- Our examiner at Linköping Institute of Technology, Björn Gudmundsson, for feedback during the project and for providing us with a workstation.
- Anders Persson of CMIV for answering questions on radiology and for providing datasets for us to experiment with.
- Our opponents Calle Hanson and Rebecca Lagerkvist for feedback and comments on the report.
- Tomas Ohlsson for providing cookies at the coffee breaks.
- Materialise for providing us with an evaluation copy of Materialise Mimics 8.
- The test person, Tobias, for putting himself through a CT scan and making the test of the software possible.

Linköping, February 2005

Björn Andersson *Martin Valfridsson*

Index

List of Figures

1 Background

Despite the introduction of DNA-analysis for identification of human remains (1997-2000) several cases exist where the deceased remains unidentified. Approximately ten percent of unknown deceased persons can not be identified by dental status or other present methods. During the year 2003 alone, seven individuals in Sweden remain unidentified. The increased travel in Europe will lead to more discoveries of foreign human remains in Sweden. In these cases, dental and medical records are often unavailable for the identification process. (Holmlund)

To decrease the number of persons that remain unidentified, 3D facial reconstruction may be used. Today, although not in Sweden, reconstructions are performed by forensic artists applying modelling clay to casts of the skulls. This method is considered unethical since it involves manipulation of the skulls. Another drawback with this method is that it is very time consuming and changes and modifications of the models are hard to do. A possible way to avoid these issues is to introduce a computer based method based on the traditional clay method.

This thesis work has been performed at Pääbo Consulting Group AB (PCG AB) in Linköping in collaboration with The National Board of Forensic Medicine's Departments of Forensic Genetics and Forensic Medicine (RMV – Rättsmedicinalverket) and the Center for Medical Image Science and Visualization (CMIV).

The underlying work for this thesis is considered a pilot project for RMV. They wanted to look into the possibilities of digitally reconstructing human faces based on discovered skeletal remains after having seen a 3D visual a reconstruction of Birger Jarl for a TV-Drama documentary created by PCG AB.

2 Overview

This thesis consists of four main parts. The first part describes the background to the project and presents the methods we have used to complete this thesis. This involves the whole process from gathering information to implementing the program.

In the second part of the thesis we give an overview of prior work and research that has been performed in the area of forensic facial reconstruction. We also present how a face is built up in order to motivate decisions we have made while implementing the software. We also give an overview of our method, in which ways it relates or differs from other methods studied.

In the third part we describe our method in detail and present the solutions we have implemented.

In the fourth part we present our results of testing the software, future development and improvements that can be made.

The report in general can be enjoyed by anyone. Some parts however go a little deeper into programming and computer graphics, and therefore require prior knowledge in these areas. Throughout the thesis some medical and technical terms that might not be known to the reader are used. For description of these terms, see Appendix A.

3 The Purpose of the Thesis

The purpose of this thesis is to explore the possibilities to eliminate problems with traditional facial reconstruction, such as time complexity, difficulties in editing the model once it is created and being able to perform a reconstruction that is considered more ethically correct than present methods. The approach used to explore these possibilities is to develop a computer based 3D modelling method for digital facial reconstruction based on computed tomography for the forensic field. A part of the prerequisites is that the method shall be implemented and tested in the 3D modelling software Discreet 3ds max.

4 Methods

In order to produce this thesis we started by studying available research and previous work done in the field of forensic facial reconstruction. We have collected information from several articles, theses and reports presented by both technical and medical researchers. To ensure the reliability of our sources we have tried to use sources that are widely referenced by other authors. We have also checked several sources for solutions to problems in order to not rely too much on any single source. Before implementing we have discussed the methods and theories with our contacts at the National Board of Forensic Medicine, Gunilla Holmlund and Calle Winskog. To get a thorough understanding for each part of the process we have not only studied the reconstruction process but also the process of data collection via computed tomography. Anders Persson of CMIV has helped us with datasets and questions on computed tomography.

We have implemented the software in MAXScript for use with 3ds max (See chapter 11 in this thesis, www.discreet.com and the reference manuals in 3ds max for further details). The implementation has been scripted in order to work as smoothly as possible together with 3ds max. We have received support and discussed our ideas on the implementation process with Michael Pääbo and Ulf Textorius of PCG AB.

In order to see if our results are satisfactory we have had help from two forensic pathologists, Johan Berge and Calle Winskog, who helped us by testing our software and giving us comments and feedback on our software.

5 Limits and Delimitations

The workflow for performing a reconstruction consists of acquiring data, pre-processing data and then performing the reconstruction. Our implementation has focused on the reconstruction process and therefore we have not implemented the two first-mentioned steps but we discuss these steps later in the report.

We have chosen to define the reconstruction process to begin once the data has been acquired and the model has been oriented and the number of polygons has been reduced in such a way that the model is manageable in 3ds max on a regular workstation.

The segmentation process is performed using external software (see chapter 14 for details) and the pre-processing of the model is performed in 3dsmax's standard user interface as this provides tools, functions and possibilities for performing a good pre-processing of the dataset. Therefore there is no use to implement this into our software.

The method is implemented in 3ds max due to a prerequisite from PCG AB. PCG AB wanted to test their ideas around 3ds max as a reconstruction tool for forensic facial reconstruction.

6 Forensic Identification

There are several methods for identifying deceased persons, some more effective than others. For example the most reliable identifications are made by simply having a relative that can identify the deceased. Photo identifications are also reliable as are identifications of characteristics on the body such as birth marks or tattoos. Other methods involve analyzing dental records, medical records or remains found on or nearby the deceased in order to identify the body. These are all methods that perform what we would like to call positive identifications where one can be certain that a correct identification is performed. Another accurate method is identification made using DNA.

Other methods can be described as elimination methods where subjects can be eliminated from a group of possible subjects. This can be done by for example being able to say that the deceased is a woman, this makes it possible to eliminate all men from the group of missing persons. The method of facial reconstruction can be used as an indicator for which subjects to eliminate.

7 Facial Prediction Methods

Caroline Wilkinson (Wilkinson, 2004) states that the most important factor affecting the face is the underlying skeleton. The skull consists of 22 bones and it is the shapes of these that provide the enormous variation between individual skulls. Basically there are two approaches to facial reconstruction, the anatomical and the tissue depth methods. These methods differ in the sense that first one tries to replicate the muscles in the face while the second approximates the tissue depth in several places on the head.

The anatomical method relies on modelling the muscles of the face and applying these onto the skull. This method is very time consuming since each individual muscle must be modelled and then placed correctly onto the skull. The tissue depth method however is based on measurements of tissue depth on a population of cadavers and is the most widely used method throughout the research studied.

7.1 Method of Choice

In order to implement a method that resembles the most common approach of 3D facial reconstruction, we have chosen to use the tissue depth method in our approach. We also find this method more suitable for implementing into 3ds max.

7.1.1 Technique in historical perspective

Forensic facial reconstructions rely on tissue depth measurement from individuals based on gender, age, sex and nutritional state. In late 19th century Him used needles with a displaceable piece of rubber which were pushed through the flesh of his cadaver specimen at right angles to the bone. The distance and the corresponding well-defined landmark were recorded and an average of the tissue distance was calculated. Him's work was extended by Kollman and Büchly in 1898 by introducing categories of nutritional state. Since then the techniques have been developed but most of the work done has its foundation in the work done in the area in the late 19th century. Measurements using X-ray have been carried out since the 1960s.
(Krogman & Iscan, 1986)

New techniques involving ultrasound, lateral craniographs, CT and MRI have been used the last decades for the collection of thickness data (Chen et. al. 2001).

7.1.2 Landmarks

Landmarks are well-defined points on the head. There are two types of landmarks, craniofacial and cephalometric. Craniofacial marks are placed on the skull and cephalometric are the corresponding marks on the surface of the skin. It is the distance between these landmarks that is measured. In facial reconstruction landmark dowels are used to illustrate this distance. Much care must be taken when placing and especially rotating the landmark dowels so that these give a good representation of the placement of the skin relative to the bone. There are a number of different landmark configurations with various numbers of landmarks. The configuration we have decided to focus on in this thesis is Rhine's configuration since this is the configuration most widely referenced to in literature. Rhine's model consists of 32 landmarks placed in suitable positions on the skull; this is illustrated in Fig. 7.1. (Archer, 1997). Unless otherwise mentioned, when referring to landmarks later in this thesis, we mean craniofacial landmarks.

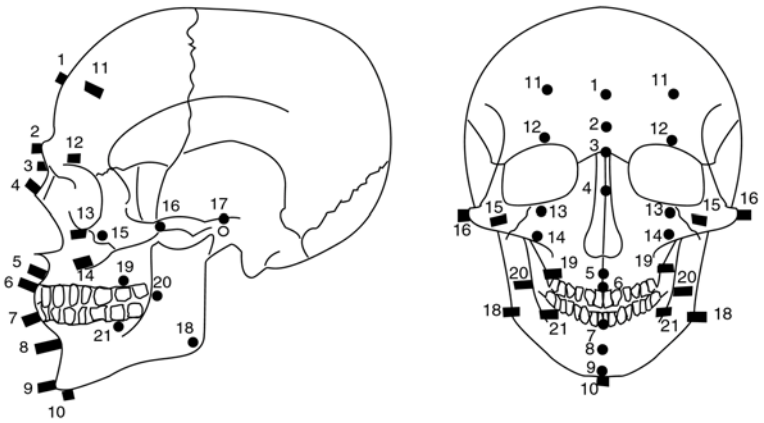

Fig. 7.1 - Rhine's Landmarks

7.1.3 Inconsistencies of Data

There are several issues with the collection of the tissue depth data. When depth measurements are acquired from cadavers it is a known fact that the structure of the tissue can be distorted within hours of death due to drying and embalming. Since the goal with forensic facial reconstruction is to produce a model as accurate as possible to the shape of the living person, this must be compensated for and taken into consideration.

Early measurements that used needles have some additional potential problems. The first is the deformation of the skin caused by the penetration of the needle. Second is the issue of finding the craniofacial landmarks through soft tissue when performing the needle insertion. According to Simon D. Michael, in Chen et al. (2001), this process requires skill and considerable training and considering the margin of error, luck must play a big part. Furthermore there is the problem of the anthropologist's individual interpretation of the highly subjective landmarks to be considered.

In addition to the issues mentioned above it should be pointed out that most measurements presented in research studies are collected from rather small populations, this gives rise to questioning of the reliability of these figures.

Wilkinson (2004) says that the ultrasound techniques are the most accurate and efficient since the tests may be carried out without any considerable danger to a living specimen. When tests are carried out with CT the risks for the living test persons must be considered. She also mentions that ultrasound makes it possible to conduct the studies having the specimen in an upright position. In opposite, tests with the MRI and CT techniques are conducted with the subject lying in a horizontal position. The soft tissue on the face tends to behave differently when the subject is lying down opposed to standing up.

7.1.4 Available Tissue Depth Data

As our focus lies on the Rhine landmark configuration we have only presented the type of data collections that tangents or closely corresponds to this configuration. Rhine has presented several datasets of different populations. All datasets are divided into sex and nutritional state (emaciated, normal and obese). The populations are American Blacks (Rhine in Archer, 1997) (Appendix B) and American Whites (Rhine in Archer. 1997) (Appendix B). These studies were conducted on cadavers and, according to Wilkinson (2004), excluded specimens that were distorted due to post mortal changes. Other applicable studies are done by Manhein et al. (2000) on black and Caucasian Americans (Appendix C) and Helmer (in Wilkinson, 2004) on white Europeans. Both studies were performed using an ultrasound technique and grouped by age. There are no available data for a Swedish or Scandinavian population known to us or to our contacts at RMV.

7.1.5 Determination of Applicable Table Data

In order to determine which tissue depth data table to use when performing a reconstruction, it is useful to determine some facts about the human skull. Such facts include race, sex, age and nutritional state.

The skull is a good indicator of the race, sex and age of the deceased. The race, for example, can be analyzed by variations in morphology (form, structure) and osteometry (relative size) of the skull. (Krogman & Iscan, 1986)

The age determination of a human skull is primarily concerned with the teeth. Gustafson suggested in 1950 that there are age related historical changes in teeth. He created a regression formula to calculate the age of an individual. Methods have been developed that are said to have the accuracy of determining the age of 75 percent of the subjects within an error of five years. When the teeth of the individual are missing, bone assessment will give age estimation to within 10-15 years. (Wilkinson, 2004)

Determining the sex of the deceased from the skull alone can be problematic. Age, environment, post mortal changes and variations between different populations may influence this considerably.

Nutritional state however is very hard to predict since this is not indicated on the skull. When no other discoveries than the skull are found, the best solution would be to create a number of reconstructions based on the different tissue depth tables.

8 Facial Structure

The basic structure of the face has evolved from the human necessity of being able to perceive, communicate and eat. The placement of the eyes and ears gives distance perception of sight and sound, the position of the nose relative to the mouth eliminates choking and the jaws and mouth region is designed for respiration, mastication and verbal communication.

This chapter presents theories on the placement of facial features based on research literature studied.

8.1 Ears

According to Wilkinson (2004), Angel and Gatliff have, in 1984, stated that the size, form and projection of the ears are attributes that are basically impossible to estimate based on the skull only. The problem is that there are no underlying bones that describe the appearance of the ears. The placement of the ears however can be determined by the auditory meatus. The opening of the ear is aligned to the opening in the cranium.

8.2 Eyes

A theory for the placement of the eyes was presented by Wilder in 1912, he stated the following: "*The position of the two canthi is almost precisely determined, the inner by the naso-lacrymal duct (lacrimal fossa) and the outer by the slightly but definitely indicated malar tubercule.*". Further studies show that these positions on the skull are most often easy to find. Regarding the depth placement of the eyeball in the socket, Wilkinson presents Wolff's strategy that says that a straight line between the superior and inferior orbital margins will touch or just miss the front of the cornea. Wilkinson (2004) presents a study performed by Fedosyutkin and Nainys, in 1993, that states that the length of the opening of the eye is 60-80 percent of the width of the orbit.

8.3 Nose

The nose is built up of the nasal bones and cartilage. There are different suggestions on how to predict the shape of the nose of a person. One theory presented by Wilkinson (2004) involves calculation of the shape of the nose based on the angle of the nasal bone. This gives a hint of the shape of the nose, but the amount and shape of cartilage is still very hard to predict by just considering these facts. Different studies performed on the correlation between the nasal bone structure and the actual nose show different results. In addition to this the nose changes its shape with time which makes the reconstruction of the nose based on the skull very hard.

Wilkinson states that general rules for reconstruction of the nose have been developed based on several studies within the area. These rules say that the nasal shape is based on the form of the nasal bones and the slope of the nasal spine reflects the slope of the nasal base. According to Wilkinson, Gerasimov has in 1971 provided the best guide to the nasal projection. He stated that "*the profile of the nose is projected by two straight lines one at a tangent to the last third of the nasal bones, and the other as a continuation of the main direction of the point of the bony spine. The point of intersection between these two lines will generally give the position of the tip of the nose*".

8.4 Mouth and Lips

The lips and mouth are important features in the appearance of a person. Some details of the mouth and lips can be determined by the structure of the underlying bones. If a person has big teeth it is also common that the lips are thick while small straight teeth tend to relate to thin lips. Gerasimov (in Wilkinson, 2004) also states that it is important to know that the lips change with age and vary widely within the same racial group. Depending on the occlusion of the teeth, the dental pattern and the shape of the jaw, the mouth shape can be determined.

A model for determining the width and position of the mouth is presented by Krogman & Iscan (1986). This model positions the corners of the mouth vertically to the centre of the eyes.

9 Human Facial Perception

When performing facial reconstruction the aim is to produce a likeliness of an individual that can be recognized by close friends or family members. Despite much research in the area of facial recognition there are still many uncertainties regarding people's methods for recognizing human faces. (Wilkinson, 2004)

In Zhao et al. it is mentioned that both holistic and feature-based information are crucial for the recognition of faces. It's also said that especially hair, face outline, eyes and mouth have been determined to be important features while studies say that the nose plays an insignificant role. Wilkinson (2004) also presents research that supports their theories. But she reserves herself to the fact that many of the tests where preformed using only frontal images and that the shape and projection of the nose was not shown. She also states that it has been shown that the face is recognized more as a whole or as interrelationship between different features than as a group of individual features.

Michael (in Chen et. al 2001) refers to studies reporting that better results in identifications from facial reconstructions are received when the viewer is allowed to use his or her imagination. Results like these have led to that features such as wrinkles, scars and hair colour are not normally added to forensic reconstructions.

10 Previous Work in Facial Reconstruction

This chapter on previous work in the area of facial reconstruction consists of two main parts, computer aided and traditional techniques.

10.1 Traditional Techniques / Manual Reconstruction

There are two major branches of manual facial reconstruction; these can be described as 3D reconstruction where clay modelling is the main approach and the 2D methods that involve drawing. These methods are described in this chapter.

10.1.1 3D Reconstruction Using Clay Modelling

The most common approach to three-dimensional facial reconstruction without the use of a computer is the clay modelling approach. The workflow of this method is presented in Fig. 10.1. Either the anatomic or the tissue depth approach is used. Using the tissue depth method involves placing landmark dowels on the predefined craniofacial landmarks on the skull (or a cast of the skull). These dowels have a size according to the tables of soft tissue measurements by Rhine discussed in chapter 7.1.4. Then modelling clay is applied and the forensic artist interpolates with clay between the different landmark dowels in order to produce a continuous skin. This method, known as the Krogman step-by-step method, produces results that can be very accurate, on the other hand it is extremely time consuming and modification of the model is not an option.

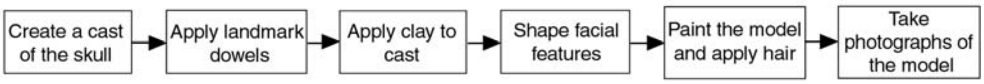

Fig. 10.1 - Workflow diagram of the manual 3D reconstruction method

The other approach of clay modelling in 3D is the anatomical approach where models of all the significant muscles on the head are modelled in order to create an anatomically correct underlying structure. The muscles are then covered with a layer of clay that represents the skin. Three-dimensional facial reconstruction using this technique requires great knowledge from the forensic artist on the placement and appearance of the facial musculature.
(Krogman & Iscan, 1986), (Archer, 1997)

Fig. 10.2 - Clay reconstruction by Oscar Nilsson

The traditional modelling techniques are also used for archaeological and historical purposes. Fig. 10.2 shows a photograph of a reconstruction of one of the crew members of the warship Vasa that sank during her maiden voyage in 1628. The reconstruction was created by Swedish model maker Oscar Nilsson and can be viewed at the Vasa Museum in Stockholm. (For the interested reader, visit Oscar Nilsson's webpage)

10.1.2 2D Techniques

This method results in two-dimensional facial and profile drawings of the reconstructed face based on the measurements previously mentioned. This method is performed by drawing contours on x-rays or photos of the skull and is basically the same technique as the three-dimensional one. Advantages with this technique is that it is substantially faster, but of course it only results in one or two images that are impossible to rotate and view from different angles.

10.2 Computer Aided Techniques

Several researchers and students prior to us have looked into the possibilities of using the computer as a tool for performing reconstructions. In order to give a brief overview of these approaches we present some interesting approaches below.

10.2.1 Volumetric Facial Reconstruction

Simon D. Michael presents, in Chen et al (2001), a method for visualizing faces called Hierarchical Volume Deformation (HVD). This method uses a reference head, H_{ref}, that is made up of the skull S_{ref} and the tissue T_{ref}.

The skull that is being reconstructed, S_{rec}, is compared to a database of reference heads. A reference head that is as similar as possible to H_{rec} is selected. The selection is made based on choosing the head from the database which matches H_{rec} as much as possible in terms of sex, age, race and cranial shape. H_{ref} is then deformed to the shape of S_{rec}, by doing this the reference tissue, T_{ref} is deformed in association with S_{ref} and produces the final reconstructed head, H_{rec}. This head should describe the original face depending on the differences between S_{ref} and S_{rec}.

Michael motivates his choice not to use the tissue depth tables by claiming that these tables are inaccurate because they are based on the average values of measurements of tissue depth on several different persons and that an average value might not necessarily represent a collection of possible tissue depths of one single person.

10.2.2 Hierarchical B-spline Interpolation

Archer (1997) has an approach to facial reconstruction that uses the Krogman step-by-step method (chapter 10.1.1). Archer points out the importance of developing a computer-based system for craniofacial reconstruction that, as much as possible, reminds of the manual methods already known to the forensic artists. Archer focuses on the use of parametric shapes and surfaces to describe the reconstructed face. By representing each curve in parametric form, each curve segment can be described as a polynomial; several piecewise polynomials approximate the parametric curve. Cubic polynomials are the most common representation since they are easily maintainable and controllable. Archer concludes that B-Splines are a good parametric representation since they offer local control and continuity at the join points. Local control means that by moving one of the control points, only parts of the overall curve is affected. Representations such as Bezier curves do not possess this property and are therefore not as easily maintained and thus not reliable enough to use in this approach to facial reconstruction. Continuity is also very important in representing surfaces since discontinuity between different segments of a curve will lead to singularities that are impossible shapes in a surface such as a human face.

10.2.3 Implicit Surfaces

The method presented by Bullock (1999) uses the Krogman method (chapter 10.1.1) for placing virtual dowels on the digitized skull. He uses emission-based implicit modelling where every polygon of the skull model emits a real value. The value is the interpolated tissue depths at the landmarks associated with the polygon. Bullock defines a method for determining which craniofacial landmarks each polygon is associated with by dividing the skull into different areas. To produce a renderable and editable mesh he polygonizes the implicit function by applying the Marching Cubes algorithm. The method does not include the possibility to directly create facial features but Bullock mentions the alternative to edit the skin in external modelling software.

11 Implementation Techniques

As mentioned in chapter 5, one of the conditions for conducting this thesis at PCG AB was to implement our software in Discreet 3ds max.

This chapter presents 3ds max, MAXScript and various tools and modifiers used in our implementation. In later chapters we describe how and why we use these tools and modifiers.

11.1 Discreet 3ds max

3ds max is most widely used as modelling software for creating visual effects, games, and design visualizations. We find it challenging and motivating to use this software in a new medical and forensic approach. 3ds max has a wide collection of advanced tools for modelling, animation and rendering some of which we have used in our implementation.

11.2 MAXScript

Integrated in 3ds max is MAXScript which is the scripting language used for creating new functions and accessing tools in 3ds max. Many of the new features implemented in each release of 3ds max are implemented in MAXScript rather than in SDK. This shows the power that MAXScript provides. (See www.discreet.com and the reference manuals in 3ds max for further details)

MAXScript is an object-oriented scripting language that every programmer with basic knowledge of object-oriented programming can easily get started with. MAXScript also provides the possibility to perform advanced programming tasks such as vector and matrix operations to create mathematically correct models.

MAXScript lets the user access most tools and functions in 3ds max. This includes modelling, animation, rendering, materials and much more. Instead of using the software as pure modelling software, tasks can be automated using MAXScript.

A feature in MAXScript is the ability to create customizable user interfaces. This allows the developer to lock functions in 3ds max that will not be used for the particular purpose in his or her software.

Like any other programming language, MAXScript supports text I/O (input and output) from external files. This can be used for retrieving data from tables produced outside 3ds max.

11.3 Modifiers and Tools

Modifiers are used in 3ds max to sculpt and edit objects. The modifiers apply internal changes on the objects and in most cases these operations are applied in local or object coordinates. The main difference between modifiers and transformations, which are the most basic manipulations in computer graphics, is that transformations are independent of the internal structure of the object and always act in world coordinates. Any number of modifiers can be applied to an object while all transforms are represented by one single transform matrix.

11.3.1 Relax Modifier

The Relax modifier changes the surface tension in a mesh by moving vertices on the mesh. Applying Relax moves each vertex toward the average position of its neighbouring vertices. A neighbouring vertex is defined as a vertex that shares a visible edge with the current vertex. Relaxing a mesh results in smoother corners and edges. Fig. 11.1 shows an example on how the relax modifier changes the appearance of a box. The leftmost box is the original, the middle box is relaxed using 10 iterations and the rightmost box is relaxed using 100 iterations.

Fig. 11.1 - Illustration of the effect of applying the Relax Modifier to a box

11.3.2 Paint Deformation Tool

The Paint Deformation tool gives the user the ability to use a brush (Fig. 11.2) to paint on the mesh and thereby push and pull vertices or relax the mesh. This tool only affects the vertices in the regions that are touched by the brush strokes. The Relax part of paint deformation works in the same way as the Relax Modifier previously described but of course only on the desired vertices. This tool can be used to level out local variations in a mesh.

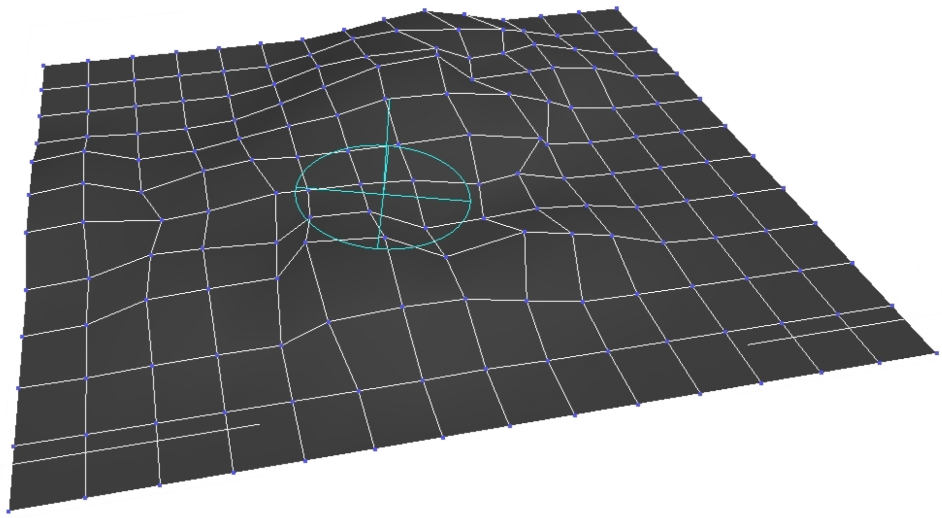

Fig. 11.2 - Illustration of the Paint Deformation Tool

11.4 Accessing and Controlling Vertices

All vertices on an object in 3ds max are stored in an array. The vertices are added to the array in numerical order when the object is created. In order to access the vertices through MAXScript, the index number for the desired vertex is used. Removing a vertex from an object gives remaining vertices with later positions in the array new index numbers. When a new vertex is inserted, no matter where on the object, this vertex is placed in the last position of the array.

Being able to locate each vertex and having control of these through their indexes is crucial in order to have full control of the mesh through scripting.

12 Our Method

Based on the research and previous work presented in prior chapters we have developed our tool for providing a possibility to create three-dimensional facial reconstructions using 3ds max. Our method relies on the tissue depth method and tries to follow the workflow of manual reconstruction. One major difference though is that our method provides mathematical calculations to describe the position of the skin on the bones and therefore provides an accurate description of the face on points such as the forehead, chin and cheekbones. Between these we perform interpolation to produce the parts of the face with underlying muscles.

12.1 Motivations

The approach we have used is to base our reconstruction on the skull, the landmark system and the tissue depth tables by Rhine (see appendix B). Additionally the approach needs user input from an expert in the area of anthropology and forensic identification. Our main concern is to produce a fully working system from having the skull of a model to generating output images of the reconstructed face.

Choices within our approach have the nature of fitting the environment of 3ds max and keeping the skinning simple and intuitive.

The method presented in chapter 10.2.1 uses reference heads. We have chosen not to use this approach since we assume that the reference models may play a too significant role in the final appearance of the reconstructed face. Also, to be able to test this method in a realistic way with a somewhat arbitrary skull includes having access to a large number of reference faces. As a collection of these faces must be said to lie outside both the financial limits and the time frame of this project this method is disregarded as a possible approach.

Using Archer's method, presented in chapter 10.2.2, involves manually placing a large number of extra landmark dowels. We find this approach to require more user input than we prefer. Looking at the results presented by Archer, the use of hierarchical B-splines in this way seems to be too independent of the underlying bone to give a satisfying result. This method only lets the skull affect the reconstructed skin at the positions of the original and extra landmarks, and not in-between. This fact confirms our assumption that the method does not produce a result that is satisfactory enough.

Our main concern with reconstructing the skin in 3ds max is to create a controllable and easy to work with mesh. Observing the work done by Bullock using implicit surfaces we find the result unsatisfying in the sense that the output mesh would be irregular and uncontrollable. Introducing the possibility to create facial features with this mesh would be hard if not impossible since this requires having a well-defined area to work with.

12.2 Workflow

When trying to replace a manual method with a computerized tool, most often an approach where the presumed user recognizes the workflow is preferable. This is a fact that Archer also points out in her thesis (Archer, 1997). Basically our method involves the same steps as the manual reconstruction process. Below is a diagram showing our method (Fig. 12.1). To compare our workflow to the clay modelling approach, see also Fig. 10.1.

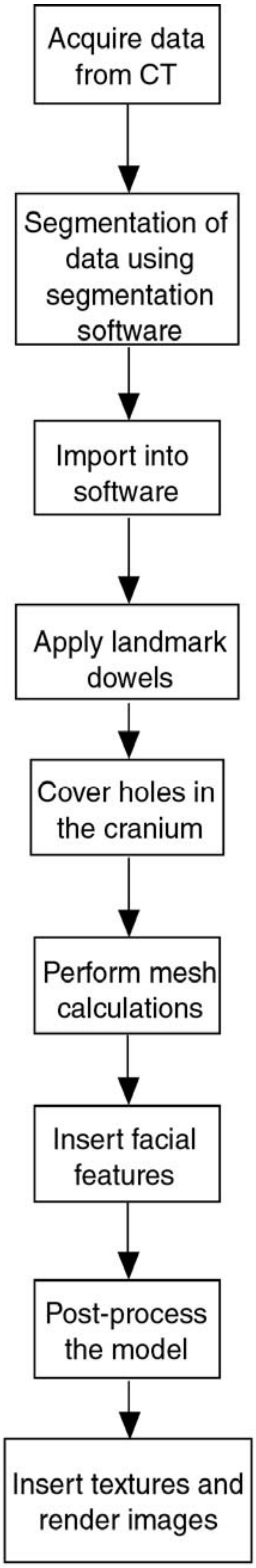

Fig. 12.1 - Workflow of our reconstruction method

1. **Acquire data from CT***
   The skull is scanned in a CT-scanner. The CT-slices are stored in DICOM format
2. **Segmentation of data***
   Segmentation software is used to edit the CT-slices in order to remove artefacts such as metal cavity fillings that give rise to errors in the images. This software is also used to produce a 3D model that can be imported into 3ds max.
3. **Import into software**
   The model is imported into 3ds max and some pre-processing such as normalization and rotation of the model is made.
4. **Apply landmark dowels**
   This is the first contact with the software we have implemented. Here the user places the landmark dowels onto the skull model using our GUI.
5. **Cover holes in the cranium**
   User input is required to specify the parts of the skull that has cavities where muscles have been attached to the cranium. The user defines these areas and the software covers the holes.
6. **Perform mesh calculations**
   Based on the landmark dowels' sizes and rotations, the placement of the skin between these is calculated. The chin and neck are also created at this point.
7. **Insertion of facial features**
   Based on the appearance of the skull, the software guides the user in creating the nose, eyes, ears and lips.
8. **Post-process the model**
   By using the tools provided in our GUI the user can make changes to the model based on his or her knowledge of the human face.
9. **Insert textures and render images**
   In order to make the model appear more lifelike, textures can be applied before rendering the images. Rendering from different angles is then performed.

* *Parts not implemented by us*

13 Data Acquisition

Our sample CT-datasets are acquired using a Siemens Somatom Sensation 16 CT Scanner (Fig. 13.1) with 0.7 mm collimation and 512 by 512 matrix.

The X-ray beam is shaped using special diaphragms known as collimators. Volume data can be reconstructed from CT-images with slice thickness equal to or larger than the collimation. For example, in our case, the volume can be reconstructed with a slice thickness of 0.7 mm or more.

Using fine collimation leads to large datasets from which accurate volumes can be reconstructed. Normally when running a patient through a CT scanner the slice thickness is much thicker than 0.7 mm, normal slice thickness is about 5 mm. (Anders Persson), (Computed Tomography - Its History and Technology)

Fig. 13.1 - Siemens Somatom Sensation 16 CT Scanner

13.1 DICOM Output

Digital Imaging and Communications in Medicine, DICOM, is the standard format for digitally storing x-ray images. A DICOM file contains a header which stores all necessary information about the x-ray examination, such as details about the patient, physician, hospital and modality. The header also specifies technical information about the dataset such as number of images in the series, the resolution of the images and the filenames.

Like any other medical x-ray examination, the examination conducted in order to use our method for 3D facial reconstruction, stores the dataset in DICOM format.

13.2 3D Volume Representation from DICOM Images

The process of generating a 3D surface from a CT-dataset is not trivial. A CT-dataset consists of a series of monochrome 2D slices. When generating the 3D volume, information from each 2D slice is processed and interpolation between the slices is performed in order to create a volume (see Fig. 13.2).

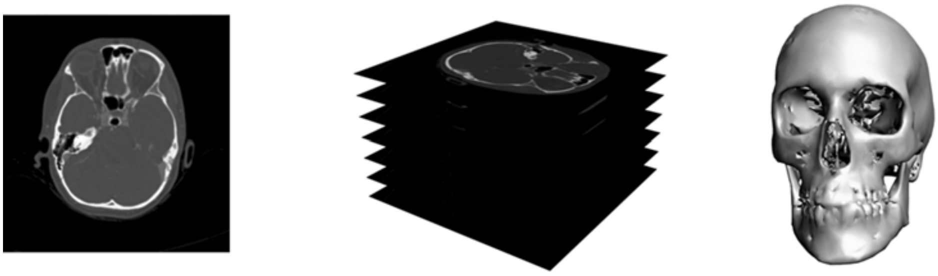

Fig. 13.2 - From DICOM to 3D volume

The Siemens software can create volume visualizations of DICOM data, but these are not importable into 3ds max since 3ds max only supports surface models. Chapter 14 contains discussions on the software requirements necessary for generating surface meshes from volumes made from DICOM and importing these into 3ds max.

14 Segmentation

This chapter describes the process known as segmentation, which involves taking the images from DICOM and performing operations to prepare the export to a 3D format.

14.1 Thresholding

A DICOM image represents different tissue densities by greyscale intensity values; bone will have high intensity while soft tissue will have lower intensity values. In order to decide which parts of the DICOM dataset that are going to represent the surface, the images must be segmented using a threshold algorithm. If the threshold is chosen too low, the surface will consist of too much soft tissue which will include the skin and muscles. A threshold set too high will lead to holes in the bone structure. The ideal threshold value is a value that removes everything but the bone tissue.

One might say that thresholding will not be an issue in this application since the only input into the CT-scanner is the skull. This is not entirely true since the skull might still have skin or muscle residue attached to it. This tissue has to be removed from the dataset using segmentation. In order to perform tests with living test persons, the soft tissue has to be removed using this technique.

In some cases it is not possible to set an overall working threshold for the whole dataset. This and the fact that some CT-images do not have sufficient resolution might lead to holes in the surface. Thresholding problems are for example likely to occur on the maxilla near the infraorbital foramen (below the eyes).

The software has to provide possibilities to check that no higher density soft tissue such as cartilage in the dataset will be interpreted as bone. This is especially important in regions where the shape of the face or facial features is dependant of the shape of the bone. In the nostril region where septal cartilage is an extension of the nasal bone, a misinterpretation of the cartilage as bone may lead to a disfigured nose. The angle of the nasal bone (or the landmark dowel placed on that bone) is used to approximate the length and angle of the nose.

14.2 Artefacts

A major problem in x-ray imaging is the artefacts that arise in x-ray images due to metallic cavity fillings in teeth. Noise in the x-ray image can also be characterized as artefacts. In order to get a working surface that will be applicable to our method, these artefacts have to be handled. Either in the segmentation process or as a pre-processing step in 3ds max prior to using our software for reconstructing the face.

14.3 Efficiency

One of our sample CT-datasets consists of 800 slices consisting of 512 by 512 pixels, each pixel represented by 16 bits. In addition to this, the header information is also included in the file which leads to a file size of more than 500kb per slice. The total size of the dataset will be roughly 450mb.

Based on the facts mentioned above it is required that the conversion software is able to handle large datasets without locking up the computer. We have come in contact with a number of different software systems that have the possibility to import DICOM and export to a 3D format such as STL for example. We have discovered that most of this software does not support the large amount of data that is required in our case and is therefore only suitable for smaller datasets.

14.4 Software for Segmentation

We have considered the possibility to develop own software for segmentation in either Matlab or using Visualization Toolkit (VTK) in connection with C++ but our conclusion is that our demands on the software, based on the facts presented above, are too high to fit the development process into this thesis. Therefore we have decided to use software provided on the market. The software we have found most useful is Materialise Mimics 8, see chapter 14.4.1 for details. (See Materialise's webpage)

14.4.1 Materialise Mimics 8

Mimics is an interactive tool for visualisation and segmentation of CT and MRI images. It can display the data in several different ways and has support for 3D visualisation and editing, morphology and boolean operations.

Mimics uses segmentation masks to highlight regions of interest. Several different segmentation masks can be used to process the images. Below is a description of the different tools that are used prior to exporting the dataset.

- **Thresholding:**
  Thresholding defines a range of grey values between the lower and upper threshold value. All pixels with a grey value in that range will be highlighted in a mask.
- **Region Growing:**
  Region growing will eliminate noise and separate structures that are not connected.
- **Dynamic Region Growing:**
  Dynamic region growing segments an object based on the connectivity of grey values in a certain grey value range.
- **Manual Editing:**
  Manual editing functions involve drawing, erasing and restoring parts of images with a local threshold value. Editing is mainly used for removing artefacts.

- **Morphology Operations:**
  Erosion, dilation, open and close are functions used to remove or add pixels from the mask.
- **Boolean Operations:**
  Boolean combinations of two segmentation masks (subtraction, union and intersection) are used for removing well defined parts of the dataset such as the bed the patient lies on.
- **Cavity Fill:**
  Cavity Fill fills internal gaps of a selected mask.
- **3D Rendering:**
  Mimics has a 3D view port in which the user can preview the dataset prior to exporting the surface.
- **Measurements:**
  Mimics can perform point-to-point measurements on both the 2D slices and the 3D reconstructions. This feature can be used to measure different parts of the face such as the size of the nose, eyes and other features.

14.4.2 File Formats

Most software that handle DICOM cannot export the 3D models to the .max format that is used in 3ds max, therefore a file format had to be found that is supported both by the segmentation software and 3ds max. There are several formats available, some more useful than others. Below follows a brief review of the different formats focusing on Mimics abilities.

Mimics has no direct support for the standard 3ds max file format .max but is able to export into STL, VRML 2.0 and DFX that all are importable into 3ds max.

- STL (StereoLithography) is a file format initially developed for stereo lithography and has become the rapid prototyping industry's standard for data transmission. It has a triangular representation of the geometry where every facet is described as three points representing the vertices and one normal direction.

- VRML 2.0 (Virtual Reality Modelling Language) is a standardized language for presenting 3D content on the web. As this is created for the web and after some none satisfactory tests we do not consider this as an alternative for an intermediate file format.

- DXF (Data Exchange File) is a file format developed by Autodesk and first used in AutoCAD. It uses tags to describe geometry. As this file format is mainly meant for constructional CAD systems and our results in trying to import DXF files from MIMICS to 3ds max was unsatisfying, we do not consider this to be an alternative.

For use in our application we have found STL to be the preferable format.

15 Implementation

This chapter discusses the implementation of the software. Throughout the chapter the graphical user interface, GUI, is mentioned. In Appendix E a number of screenshots are included in order to give the reader an understanding of the layout and design of the GUI.

15.1 Apply Landmark Dowels

As discussed in chapter 12 our method is based on the placement of landmark dowels onto the skull. We have implemented a GUI that allows the user to place the landmark dowels onto the skull in a way that very much resembles the traditional approach. The GUI guides the user through the placement process by providing guide images where each landmark is presented.

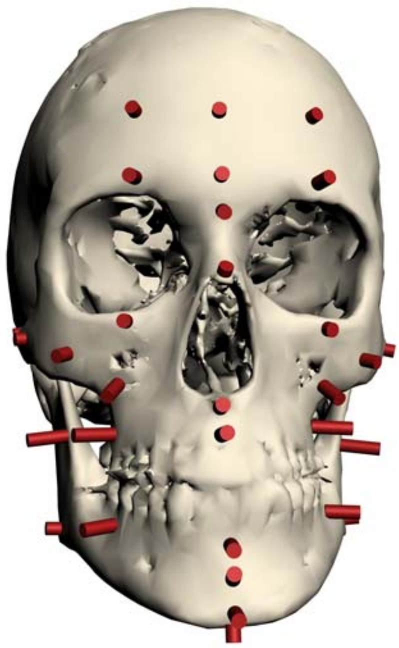

Fig. 15.1 - Landmarks placed on skull

By default the landmark dowels are defined to have a direction that is normal to the point where they land on the skull. This direction is not always completely correct since the correct direction is normal to the skin where the needle was once inserted (see chapter 7.1.1). This is not necessarily the same direction as the normal direction on the skull. In order to compensate for this our GUI provides the possibility for the user to rotate the landmark dowels into a satisfactory direction.

The lengths of the landmark dowels are imported from external data files using the I/O methods supported by MAXScript. One data file contains the name and a short description of where to place each landmark. Other files contain the lengths of the landmark dowels. The user can choose between different tables depending on the properties of the skull that have been determined (see chapter 7.1.5). Fig. 15.1 shows a skull with landmark dowels applied using our software.

Fig. 15.2 - Holes in the skull

15.2 Cover Holes in the Skull

Fig. 15.3 - Errors in mesh due to holes in the skull

A major problem when applying our mesh calculation method occurs when no points of intersection between the projected ray and the surface of the skull can be found. These artefacts occur due to the openings in the skull. These openings are located in areas where muscles are the major underlying tissue for example at the temples and on the cheeks (Fig. 15.2). See Fig. 15.3 for an illustration of the artefacts. In order to prevent these artefacts we have implemented a method for covering such holes in the skull. The user applies a spline onto the skull where the muscle would be attached. The spline defines the outlines of the openings and is then used to create a surface that covers the opening.

15.3 Perform Mesh Calculations

This part of the implementation was the most challenging part of the project. We discussed and tried several approaches before finding a method resulting in a satisfying result. Among the ideas we looked into was using the existing skull mesh and expanding it locally according to the size of nearby landmark dowels. Another approach was building up triangles using the landmark dowels as vertices. The first approach that showed a promising start used splines to build up a sort of chicken wire. From the landmark dowels, extra landmark dowels were interpolated. By connecting the landmark dowels and the interpolated dowels, a net of squares could be built up. In addition to the size of the landmark dowels, the direction of these would also affect the shapes of the splines. The next step of the algorithm would be to create additional splines between the already existing ones. An advantage with this method would have been the possibility to iteratively control the density of the wire net, hence the accuracy of the mesh. Unfortunately a few difficulties arose. No way was found to create a controllable mesh due to vertex numbering problems (see 17.1.4). Also, this method was highly dependent on finding points on the skull mesh. This was done by accessing a built in ray casting function in 3ds max. On a general skull mesh problems would occur due to the fact that the rays projected sometimes miss faces on the mesh. When these errors occurred, the points were approximated using the correctly calculated nearby points. When a series of consecutive errors occur, the error is accumulated which makes this approach much too unreliable. The mentioned problems were considered too severe and since no solutions to them were found, this approach was abandoned.

Our current method involves beginning with a simple geometric object and projecting its vertices onto the skull (Fig. 15.4). Since the transition from a primitive object to a mesh results in a predictable vertex numbering in 3ds max we get a much more controllable mesh. Unlike our prior approach, errors by this method are only locally dependent on the ray casting function.

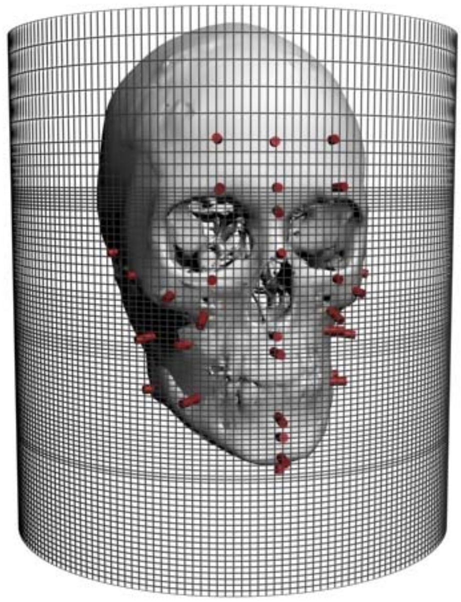

Fig. 15.4 - Cylinder mesh

The first step in the algorithm is to create a cylinder mesh placed around the skull model. The second step is to project each vertex along a straight line towards the origin of the current cylinder segment. The last step is to find the final position for the vertex by interpolating between the nearby landmark dowels. The amount that each landmark dowel affects the direction of a specific vertex displacement is relative to the squared distance between the landmark and the position of the vertex given by:

$$direction = \left\| \sum_{i=1}^{N} \frac{dir_i}{dist_i^2} \right\|$$

where dir_i is the direction of the ith contributing landmark dowel, $dist_i$ is the distance from the same landmark dowel to the projected vertex position on the skull. N is the number of contributing landmarks. The corresponding distance that the vertex is to be moved in the above direction is

$$distance = \frac{\sum_{i=1}^{N} \frac{len_i}{dist_i^2}}{\sum_{i=1}^{N} \frac{1}{dist_i^2}}$$

where the additional notation len_i is the length of the ith landmark dowel.
The collection of landmark dowels that will affect each vertex of the skin mesh is decided depending on their placement on the skull. As of now we just make a simple subdivision of the skin; the right and the left lateral vertices. They are affected by the frontal and right lateral landmarks and the frontal and left lateral landmarks respectively. Finer subdivision could be done, see chapter 18.2.

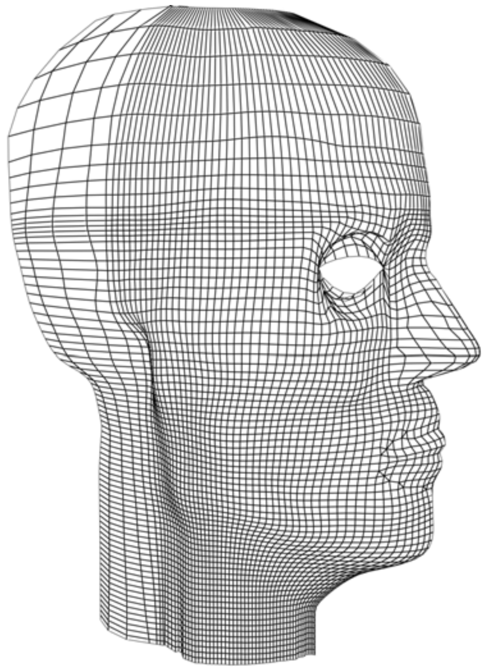

Fig. 15.5 - Reconstruction mesh

In order to be able to run the application on a standard PC workstation the number of calculations performed has to be taken into consideration. The most time consuming calculations of our process occur when the mesh is created. The time consumed is directly related to the number of vertices in the mesh. In order to reduce the computing time we have used different resolutions for the mesh on different positions on the head. This is shown in Fig. 15.4 and Fig. 15.5. We have chosen to use low resolution in the back of the head and increase the resolution on significant parts of the face such as the areas around the eyes, mouth and chin. These are areas where large variations and many details on a human face occur. We have defined the number of rows of vertices between different landmarks. These rows are then evenly distributed between the chosen landmarks. Note the rows in Fig. 15.4 that fall below the skull; these are the rows that make up the neck of the head in Fig. 15.5.

15.4 Insert Facial Features

Facial features such as mouth, eyes, nose and ears are important features when distinguishing one person from another. The appearance of these features cannot be predicted just based on the skull. Therefore we have implemented rather neutral features and given the user the possibility to manipulate features based on his or her artistic skills and the knowledge of the specific skull.

Our first approach was to have libraries of eyes, mouths, ears and noses and let the user choose from these. We found that this did not produce a satisfactory result in the case of the nose for example. Therefore we have used different approaches for the different features, see below.

15.4.1 Ears

Based on our preliminary studies and discussions with Winskog we have come to the conclusion that the most suitable method for creating ears on our model is to use pre-modelled ears and attach these onto our model. We base this decision on the difficulties in predicting the shape, size and appearance of the ears by just considering the skull. Furthermore, the complex geometry of the ears, describing these using parametrical functions is not an option. We have chosen to use a neutral model of the ears in order not to draw too much attention to them but still being able to present a head that does not lack any features.

The ear models are scaled according to the positions of the eyebrows and the lower edge of the nose. We have found these positions to be good references when approximating the size of the ears. The ears are positioned according to the landmark dowel which is placed adjacent to the opening in the cranium known as the auditory meatus. In order to take advantage of the forensic artist's expertise the GUI lets the user scale and rotate the ears by using sliders.

15.4.2 Eyes

Due to the complexity of the bone structure, defining and locating the eye socket has been determined to be very hard using automated algorithms. Therefore we let the user define the outlines of the socket by simply using a Paint Tool to paint the vertices around the socket (Fig. 15.6). When the vertices are selected, the algorithm finds all the vertices enclosed by the selection. The vertices are then divided up into different arrays depending on their position in the socket. The most interesting array is the array that defines the opening between the upper and lower eyelids, further on referred to as *openingArray*. In this case we have to ignore the problem with adding vertices to the mesh (see chapters 11.4 and 17.1.4 for more details on the vertex numbering problems) because now an opening in the mesh is needed. The vertices in the *openingArray* are duplicated and one set of the vertices is

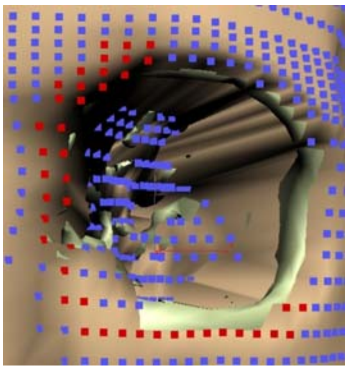

Fig. 15.6 - Paint selection in progress

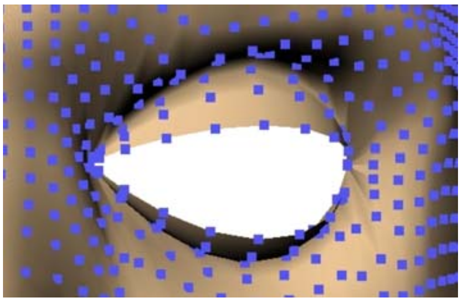

Fig. 15.7 - Open eye

associated with the upper eyelid and the other set associated with the lower eyelid. Now the mesh is split between the vertices in the *openingArray* and by moving the vertices belonging to the eyelids up or down an opening between the eyelids is created (Fig. 15.7).

Using spherical coordinates the eye is shaped depending on the parameter inputs that the user makes in the GUI. The user can change the appearance of the eye by changing different parameters such as radius, size and shape.

Based on the shape of the eyelids an eyeball is created from a plane that is shaped to fit the eye opening by using the parameters from the GUI as input.

15.4.3 Nose

Our approach to creating the nose uses Gerasimov's theory (chapter 8.3) in order to suggest a nose, but we have also implemented possibilities for the user to manipulate the shape and size of the nose through our GUI.

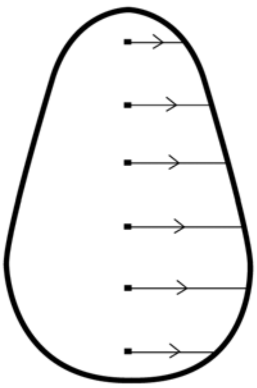

Fig. 15.8 - Locating the nose vertices

The nasal cavity is the cavity that is most easily located on the skull since it is usually well defined by sharp edges. Our method finds all the vertices on a virtual line between the landmark just above the nose and the landmark just below the nose. From each of these vertices we then search the vertices on both the right and the left side until we find a sharp edge (see Fig. 15.8). This is determined by finding a large difference in position between two adjacent vertices in the array. We then store the vertex numbers of all the vertices inside the cavity and use these to define the nose. We calculate the positions of the vertices between the middle line and the located edges. The positions are calculated by mathematical functions with parameters that regulate the length, direction and falloff of the nose. These are the parameters discussed earlier that the user can change.

15.4.4 Mouth and Lips

Using Krogman's theory on the placement of the mouth presented in chapter 8.4 and the placement of the landmarks just above and just below the teeth, we define which vertices make up the mouth and lips. We define a rectangular area containing all the mouth vertices. This area is then shaped into a pair of lips.

An issue that has to be taken into consideration when creating the mouth is the fact that the shape of the mesh in this area is affected by the underlying teeth. In order to eliminate the tooth structure on the mesh we relax the mesh in the selected area. This operation is performed by accessing the Relax Modifier (see chapter 11.3.1) in 3ds max through MAXScript.

In Fig. 15.9 a sequence of the mouth creation process is shown. The leftmost image shows the original mesh, the middle image shows the mesh after relaxation and the rightmost image shows the mouth created on the relaxed mesh.

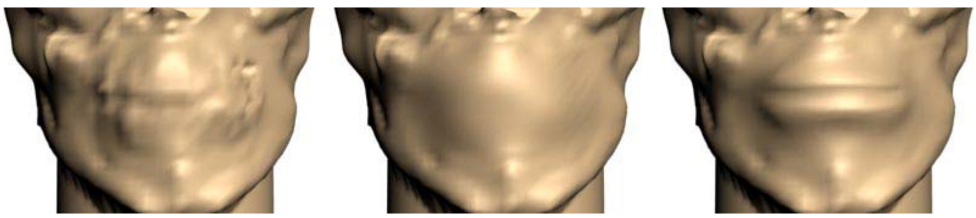

Fig. 15.9 - Effects of the Relax Modifier applied around the mouth

15.5 Post-Process the Model

After the software has performed the calculations and presented the first draft of the reconstructed model the user gets the possibility to manually manipulate the model into desired shape and appearance. In our GUI we present the user with the Paint Deformation Tool (see chapter 11.3.2).

15.6 Apply Textures

Applying textures to the model gives the model a more realistic look. As presented earlier, some of the literature we have studied suggest not to create a too realistic model but to leave parts for the beholder to consider in his or her imagination. Therefore we have put little effort in the texturing aspects of the reconstruction process. There are several possibilities in 3ds max for texturing models, which we recommend to use.

15.7 Render Images

In order to present the images of the reconstructed faces to the general public, that do not have access to 3ds max, rendering of the images has to be performed. We have used the built-in renderer in 3ds max and have implemented an interface in our GUI. In the GUI the user gets to set the number of angles he or she wishes to render the image from and also whether the rendering should result in a JPG-image or an AVI-video sequence. The images and/or video sequence are then rendered in the desired number of angles and saved in the working directory.

15.8 Graphical User Interface

3ds max is a complex software with possibilities to perform many different tasks. Providing such possibilities often lead to complicated user interfaces that contain an immense number of buttons, menus and tools. One possibility that is provided in 3ds max is the possibility to remove and adapt the user interface to suit different users.

In our software we have chosen to remove most of the menus, buttons and toolbars in order to provide our users with a more intuitive interface that is adapted to fit our implementation. We have added own menus, buttons and toolbars that the everyday user of 3ds max will never see.

Fig. 15.10 shows a screenshot from the GUI (more screenshots can be found in Appendix E). We have focused on guiding the user all the way through the reconstruction as intuitively as possible. The tabs at the top of the GUI symbolize each step in the reconstruction. These tabs are locked to the user until each prior step is completed. For example, the user cannot apply skin to the skull before all 32 landmarks are placed.

At the bottom of the GUI we have put buttons for the tools we find useful when performing the reconstruction, this toolbar is visible throughout the reconstruction. The more experienced 3ds max user may miss some tools and features that are normally available in the software. Our user interface can be overridden by pressing the "Standard UI"-button and the standard user interface of 3ds max will be available to the user.

Each time the user proceeds to a new step, the 3ds max file is saved so that it can be reloaded if the user wishes to go back at a later point in time.

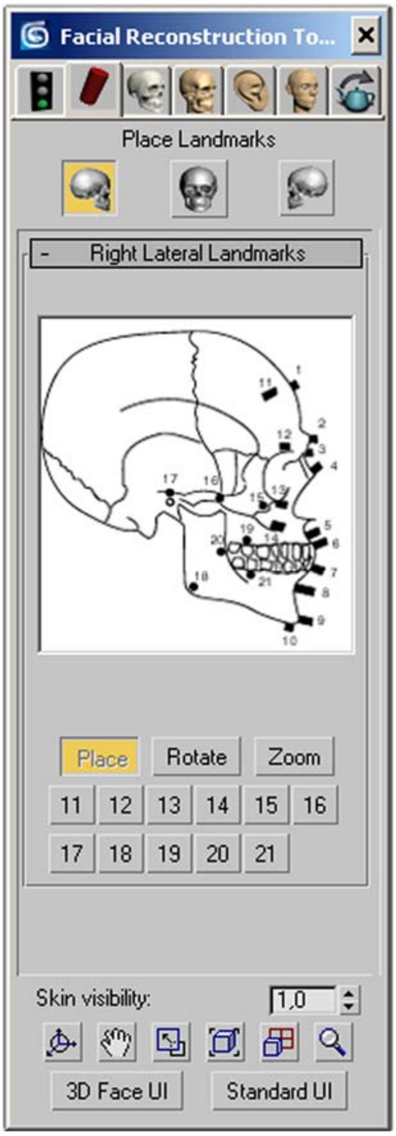

Fig. 15.10 - Screenshot of the graphical user interface

16 Clinical Test

After having finished the reconstruction software we conducted a test with two forensic pathologists, Calle Winskog and Johan Berge, from the National Board of Forensic Medicine. Prior to the test, a voluntary test person had been scanned in the CT-scanner at CMIV and photographs were taken.

None of the pathologists had prior practical experiences of 3ds max or of forensic facial reconstructions. Winskog has continuously followed the work on this thesis and Berge has gotten information from Winskog prior to the tests in order to get an understanding of the software and the reconstruction process. As technical support, Valfridsson assisted the pathologists during the reconstruction. In order to conduct the test as correctly and with as much likeliness to a sharp situation as possible, neither the pathologists nor Valfridsson received any information about the test person prior to the test.

The pre-processing of the data was performed by Andersson who, due to his knowledge about the test person, only took part in the reconstruction as a spectator. The pre-processed skull model used in this test is shown in Fig. 16.1.

Fig. 16.1 - Pre-processed skull model

The test started with an hour of introduction of the software, the pathologists then got to perform one reconstruction each. The pathologists had to rely on their expertise in examining and identifying deceased persons when choosing which tissue depth table to be used for the reconstruction.

The results of the clinical study are presented in chapter 17.2.

17 Results and Conclusions

Forensic identification and to our concern, forensic facial reconstruction are areas where much research has been conducted in the past and certainly much more research will be made in the future. Many of the sources we have studied, including the professionals we have come in contact with during the project, agree on the difficulties in the area concerning facial reconstruction. Due to the complexity of the nature's power and ability to create each and every person different, one can conclude that no mathematical function will ever be able to describe the reconstruction process of the human face.

Two types of results have been made during this project, one is the conclusions that we have been able to draw considering our knowledge and experience in programming and forensic sciences, the other consists of the actual reconstruction results when testing the software together with personnel from RMV.

17.1 Implementation Conclusions

In this section we explain and present some of the difficulties experienced when implementing the software.

17.1.1 User Input

When first beginning to work on this thesis we had thoughts on developing a more or less automatic process with limited user input. After the study of previous work and some experimentation with the software we realized the importance of the artistic input in order to create a good reconstruction. Knowledge acquired through medical studies and working experiences in the area of facial reconstruction can simply not be completely replaced with computer software.

17.1.2 MAXScript

After having worked with MAXScript we have found some drawbacks with the language. MAXScript has insufficient documentation and many problems cannot be resolved by simply using the reference manual. Therefore we have had to consult the user's forum on Discreet's webpage for rather simple questions. Another problem with the scripting language is the inconsistency of the syntax in some cases. Some examples are shown below.

For example:

```
m_lmPlaceBtn.state = true
m_lmPlaceBtn.enabled = true
```

can be done, but

```
m_lmPlaceBtn.changed = true
```

cannot, in this case

```
m_lmPlaceBtn.changed true
```

is expected.

Since the debugging possibilities provided in the MAXScript editor are very limited, syntax errors like these are very hard to locate.

While creating the GUI we have understood that MAXScript may not be the best language to create interfaces in. Many interface components that are available in other languages such as Java or Visual Basic are not available in MAXScript. Therefore the design and function of the GUI will be rather limited in some aspects by simply using MAXScript. We have chosen to import ActiveX components into our GUI to include some features not available in MAXScript.

When trying to implement the Paint Deformation tool in our GUI we have found that the possibility to access this tool through MAXScript is not implemented in the current version of 3ds max. We have contacted a developer at Discreet who explained that a mistake has been made and this feature will be implemented in future releases of 3ds max.

17.1.3 Adding Facial Features to the Mesh

While testing different approaches on how to implement and attach facial features to the model we came to the conclusion that attaching separate objects often led to shading problems when rendering the images. The reason for this is that discontinuities occur in some of the boundaries. Creating holes in the mesh and then adding the models and adapt the boundaries by interpolating the normals would create a satisfactory result, but this leads to problems in the vertex numbering. Since the numbering of the vertices is crucial for controlling the mesh this approach did not work either. Removing a vertex from the mesh affects all the vertices with higher vertex number than the removed one and adding new vertices anywhere on the mesh gives the new vertices vertex numbers starting from the vertex with highest vertex number in the mesh.

17.1.4 Vertex Numbering

The fact that inserting and removing vertices result in rearranging the vertex array gives rise to a few problems. When for example inserting a vertex somewhere on the object in order to create a more detailed mesh, two vertices lying next to each other are not given indices after each other in the vertex array. This results in problems when accessing multiple vertices through MAXScript.

For example:

```
for i = 1 to 10 do
(
    $object.verts[i].pos = $object.verts[i].pos + [0,0,1]
)
```

would move 10 vertices that are placed next to each other 1 unit in z-position (Fig. 17.1). An object with 200 vertices results in the length of the vertex array being equal to 200.

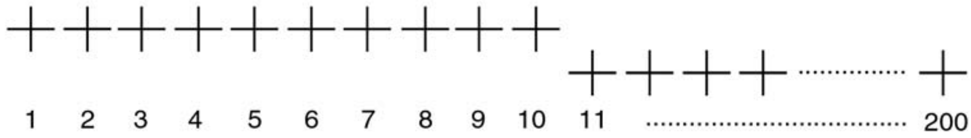

Fig. 17.1 - Vertex array with moved vertices

Inserting a vertex between vertex 4 and 5 and then performing the same loop again would result in all vertices between the first and eleventh vertex being moved while the newly inserted vertex is now placed on position 201 in the array and will therefore not be moved (Fig. 17.2).

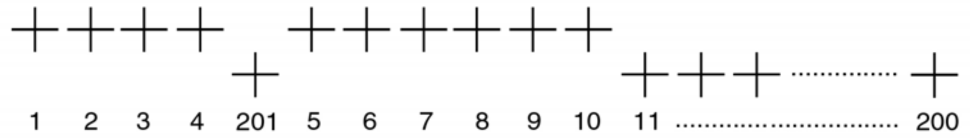

Fig. 17.2 - Vertex array with new and moved vertices

The loop for performing the correct transform to the vertices would have to look like:

```
for i = 1 to 9 do
(
    $object.verts[i].pos = $object.verts[i].pos + [0,0,1]
)
$object.verts[201].pos = $object.verts[201].pos + [0,0,1]
```

which would work if the number of inserted or deleted vertices was known in advance, but this is not always the case.

This explains the importance of keeping the consistency of the mesh throughout the implementation.

17.2 Reconstruction Results

Testing the software was very interesting and seeing that the forensic pathologists managed to run the software without extensive help from

Valfridsson was a great success for us. Fig. 17.3 shows Winskog performing the test with assistance from Valfridsson.

The introduction to the software took one hour and the reconstruction took approximately two hours to perform. A majority of the time was spent on placing the landmark dowels and manipulating the mesh into a satisfactory result.

17.2.1 Working with the GUI

None of the forensic pathologists had ever used 3ds max prior to the test which put extra pressure on our GUI. Winskog expressed his appreciation for the design of the GUI and found it easy to work with. He thought the GUI provided good guidance through the process.

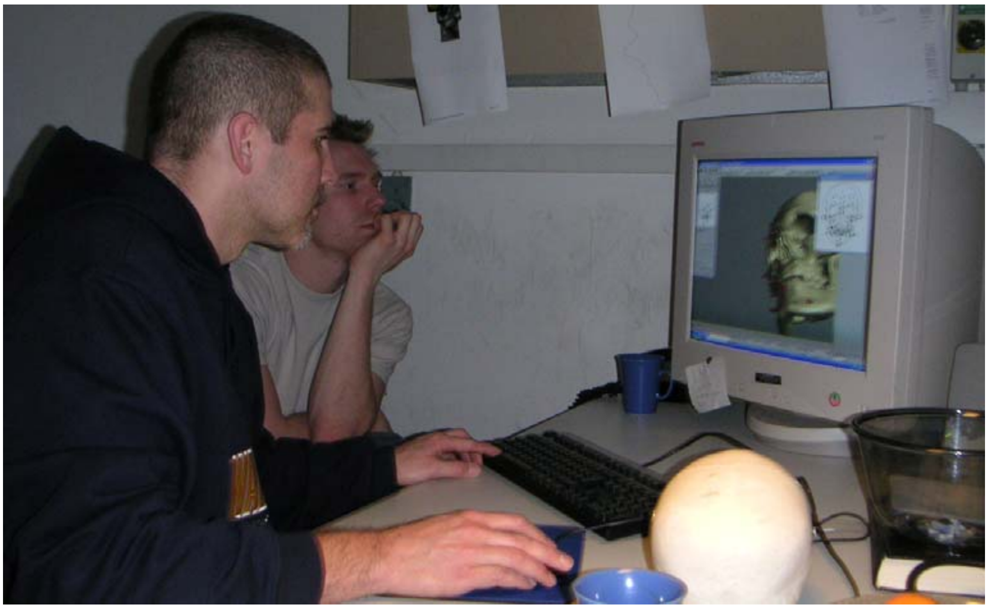

Fig. 17.3 – Winskog performing the test with guidance from Valfridsson

17.2.2 Choosing Tissue Depth Table

After having examined the skull model for a few minutes, independently of each other, both Winskog and Berge drew the conclusion, based on the prominent forehead and the shape of the skull, that the skull most likely belonged to a white male. Both Berge's and Winskog's definite opinions were that determining the nutritional state of the test person was not possible based only on the skull; they therefore, both, decided to use the tissue depth table describing a white male of normal build.

17.2.3 Manipulating the Mesh

Winskog explicitly expressed his appreciation for the paint deformation tool and thought that this method was excellent for manipulating the mesh in desired areas.

17.2.4 Visual Results

Fig. 17.4 and Fig. 17.5 show the reconstructions performed by Winskog and Berge. Fig. 17.6 shows a photograph of the test person.

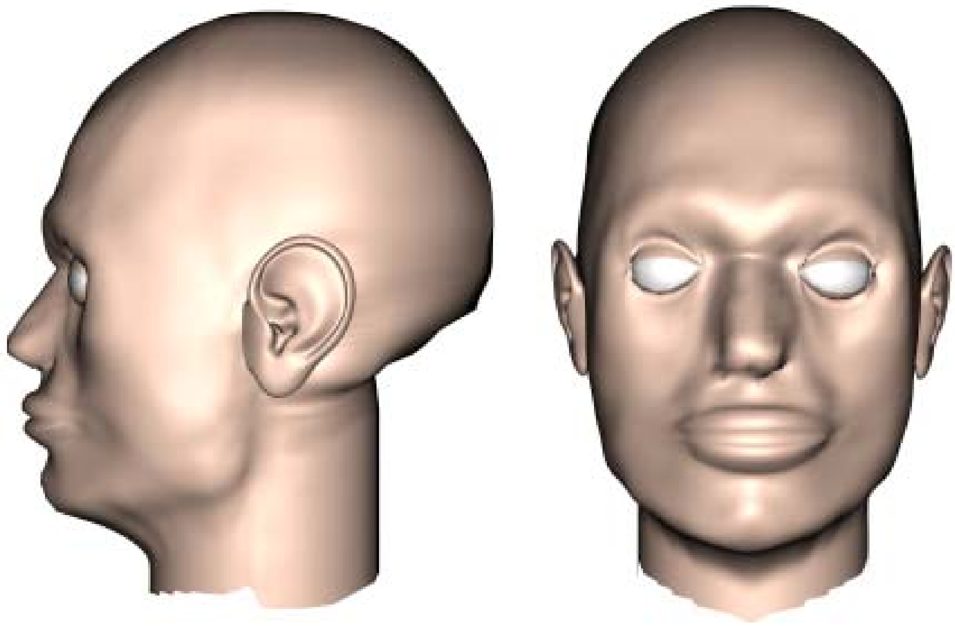

Fig. 17.4 - The result of Winskog's reconstruction

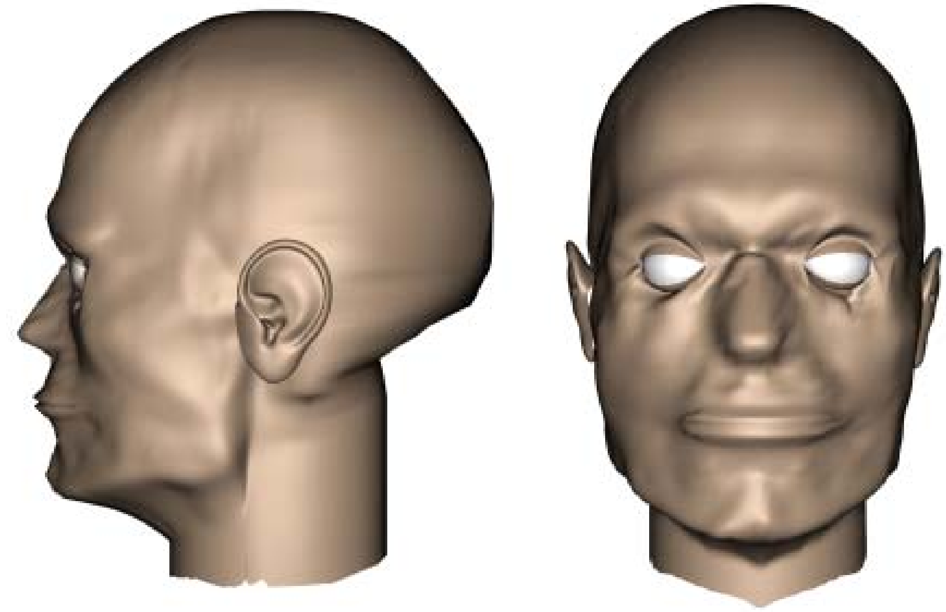

Fig. 17.5 - The result of Berge's reconstruction

Fig. 17.6 - Photo of the test person

17.3 Comments on the Results

The visual results show that it is possible to use our software in combination with 3ds max for creating a forensic facial reconstruction. The tests show that this method is substantially faster than the traditional approach. Also, we have shown the possibility of editing the completed model. Since no manipulation is done to the actual skull, we have also managed to eliminate the ethical issues of the traditional approach.

We find that the reconstructions tend to create persons with hollow cheeks. Considering the results from the test of the software we confirm the theories that the appearance of facial features is hard to determine based only on the skull.

We are pleased with the result that we have produced. The feedback we got from the forensic pathologists when using our software was even more positive than we had imagined.

We believe that a forensic artist with prior experience of facial reconstruction will be able to use this software to perform a reconstruction that resembles the original person just as much as reconstructions performed with the traditional clay modelling approaches, but in a fraction of the time.

18 Future Work

During a study and implementation process like the one presented in this thesis many thoughts and ideas arise. Due to the time frame and limited prior knowledge and experiences within the area, some thoughts and ideas will stay at being just thoughts and ideas. This is why we want to spend this last chapter of the thesis presenting some of our thoughts on what more could be done in order to bring new knowledge into the field of forensic facial reconstruction.

18.1 Locating Regions of Interest on the Skull

As presented earlier in the thesis we let the user define regions on the skull where our skinning algorithm does not work. We have not found a suitable method for automatically locating these areas. Future work could look into the possibilities of mathematically locating areas such as the eye sockets, muscular attachments and other openings in the skull. Better algorithms for the interpolation of these areas would also be of interest.

18.2 Improved Interpolation Algorithm

Since the landmarks are not evenly distributed over the face and because of the wide complexity of the human face structure, the process of deciding which areas of the skin that will be affected by which landmarks is difficult. This decision requires extensive knowledge in the areas of facial anatomy and interpolation techniques and can be a starting ground for future work.

18.3 Tissue Depth Data from more Suitable Populations

Discussed earlier are the different tissue depth data studies available today, many of which could be more accurate. We know from our studies and contacts that more comprehensive studies could be made and we assume that these are being made as this thesis is produced. For example, some pathology laboratories around the world are about to start performing virtual autopsies using CT scanners. If these examinations are conducted with high enough resolution, data could be used for collecting tissue depth data from every deceased person that is examined. Even more desirable would be acquiring data with the use of ultrasound on living persons. This would give a large collection of data acquired from many different people resulting in more reliable values and the possibility to use data that is more adapted to local populations.

18.4 Usage of Other Landmark Configurations

Due to the fact that several landmark configurations exist and to requests from RMV, we have made sure that adaptation of our software in order to use other landmark configurations is possible. This would require some changes in the code, but no extensive manipulation of the method. The changes would involve adding or removing buttons from the GUI for example.

18.5 Implementation as Stand-alone Software

The method we have implemented is strictly developed for Discreet 3ds max. Future work could include an investigation of the profitability in performance and other factors as result of an implementation as stand-alone software.

18.6 Implementation of the Entire Process

Included in the implementation presented in this thesis is only the reconstruction process, not the segmentation or acquisition processes where we have recommended separate software. One improvement or addition to the software in order to produce a solution for the whole process is to implement software that handles the raw data from the CT scanner and lets the user work with this data without the use of separate software.

18.7 Extensive Test Study of the Software

Regardless of whether the implementation is stand-alone or implemented into present modelling software, more extensive testing of the software has to take place prior to using the software in sharp situations in order to determine the credibility of the method. Through discussions with our professional contacts we have come up with a method for performing the test. Basically the test study would involve a number of volunteer subjects of different age and sex. These persons would go through a CT scan of the head and would also be photographed. A forensic artist would then perform the reconstruction of the faces using the software. The reconstructions along with the photographs of the subjects would be presented to a panel of uninitiated persons whose task would be to pair the reconstructed faces with the photographs.

18.8 Usage of the Software

One of the most terrible disasters as of today is the Tsunami that struck south-east Asia around Christmas of 2004. The media coverage of this catastrophe has focused much on the difficulties in identifying all the human remains found in the area. Many of the bodies will most likely never be identified due to the severe damage caused by injuries and decomposition. Performing manual reconstructions on such an amount of skulls is not an option since this would involve many years of hard work. Perhaps a computerized method could be used in some of the cases. But known to us, no such method, that has been thoroughly tested and verified, exists today.

19 References

19.1 Books

Chen, Min & Kaufman, Arie & Yagel, Roni (2001). *Volume Graphics*. Springer-Verlag.
ISBN 1-8523-3192-5

Farkas, Leslie G. (1981). *Anthropometry of the Head and Face in Medicine*. Elsevier.
ISBN 0-444-00557-9

Krogman, Wilton Marion & Iscan, Mehmet Yasar (1986). *The Human Skeleton in Forensic Medicine, Second Edition*. Charles C Thomas – Publisher.
ISBN 0-389-05224-7

Sobotta, Johannes (1983). *Atlas of Human Anatomy 1, Head, Neck, Upper Extremities*. Urban & Schwarzenberg.
ISBN 0-8067-1710-6

Wilkinson, Caroline (2004). *Forensic Facial Reconstruction*. Cambridge University Press.
ISBN 0-521-82003-0

19.2 Papers, Articles, Theses & Brochures

Archer, Katrina Marie (1997). *Craniofacial Reconstruction Using Hierarchical B-Spline Interpolation*. The University of British Columbia.
[Thesis, Master of Applied Sciences]

Bullock, David William (1999). *Computer Assisted 3D Craniofacial Reconstruction*. The University of British Columbia.
[Thesis, Master of Science]

Fromherz, Thomas (1997). *Face Recognition: a Summary of 1995 - 1997*. Berkeley University.
[Paper]

Manhein MH, Listi GA, Barsley RE, Musselman R, Barrow NE, Ubelaker DH. (2000). *In vivo facial tissue depth measurements for children and adults*. Journal of Forensic Sciences 2000;45
[Paper]

Siemens Medical Solutions (Date missing). *Computed Tomography - Its History and Technology*. Siemens Medical Solutions
[Brochure]

19.3 Webpages

DICOM, *http://www.dicomanalyser.co.uk/html/introduction.htm.* Accessed 2005-02-09

Discreet's webpage, *www.discreet.com.* Accessed 2005-02-09

Materialise's webpage, *www.materialise.be.* Accessed 2005-02-09

Nilsson, Oscar. *www.odnilsson.com*. Facial reconstructions by Swedish artist. Accessed 2005-02-09

19.4 Interviews & Supervisors

Berge, Johan
MD. Forensic Pathology
The National Board of Forensic Medicine
Department of Forensic Medicine
Linköping, Sweden

Gudmundsson, Björn
Lecturer
ITN
Linköping University
Linköping, Sweden

Holmlund Gunilla,
PhD. Forensic Genetics
Associate director
The National Board of Forensic Medicine
Department of Forensic Genetics
Linköping, Sweden

Persson, Anders
MD. Radiology
Manager
Center for Medical Image Science and Visualization
Linköping University
Linköping, Sweden

Pääbo, Michael
CEO
Pääbo Consulting Group AB
Linköping, Sweden

Winskog, Calle
MD. Forensic Pathology
The National Board of Forensic Medicine
Department of Forensic Medicine
Linköping, Sweden

Appendix A – Dictionary

Anthropologist – Person who studies anthropology, the science of the human race

Auditory meatus – The passages in the outer ear that transports sound

Cartilage – The strong white substance found between the joints in the body

Cephalometric – Associated with the surface of the skin

Craniofacial – Associated with the surface of the cranium

Craniograph – An instrument for outlining the skull

CT – Computed Tomography

Infraorbital – Below the orbit

Landmark dowel – Marker to represent the distance between a craniofacial landmark and the corresponding cephalometric landmark in facial reconstruction.

Maxilla - The largest bones of the face and form the whole of the upper jaw

MRI – Magnetic Resonance Imaging

Osteometry – The measurement of bones

Appendix B – Tissue Measurement by Rhine

Table B1. Tissue depth means (mm) for American Caucasian adults of different weights.

		Emaciated		Normal		Obese	
		Female *(N = 3)*	Male *(N = 3)*	Female *(N = 19)*	Male *(N = 37)*	Female *(N = 3)*	Male *(N = 8)*
Point Numbers & Descriptions		Mean	Mean	Mean	Mean	Mean	Mean
1	Supraglabella	2.50	2.25	3.50	4.25	4.25	5.50
2	Glabella	4.00	2.50	4.75	5.25	7.50	7.50
3	Nasion	5.25	4.25	5.50	6.50	7.00	7.50
4	End of Nasals	2.25	2.50	2.75	3.00	4.25	3.50
5	Mid Philtrum	5.00	6.25	8.50	10.00	9.00	11.00
6	Upper Lip Margin	6.25	9.75	9.00	9.75	11.00	11.00
7	Lower Lip Margin	8.50	9.50	10.00	11.00	12.25	12.75
8	Chin-Lip Fold	9.25	8.75	9.50	10.75	13.75	12.25
9	Mental Eminence	8.50	7.00	10.00	11.25	14.25	14.00
10	Beneath Chin	3.75	4.50	5.75	7.25	9.00	10.75
11	Frontal Eminence	2.75	3.00	3.50	4.25	5.00	5.50
12	Supraorbital	5.25	6.25	7.00	8.25	10.00	10.25
13	Suborbital	4.00	2.75	6.00	5.75	8.50	8.25
14	Inferior Malar	7.00	8.50	12.75	13.25	14.00	15.25
15	Lateral Orbit	6.00	5.00	10.75	10.00	14.75	13.75
16	Zygomatic Arch, midway	3.50	3.00	7.50	7.25	13.00	11.75
18	Supraglenoid	4.25	4.25	8.00	8.50	10.50	11.25
19	Gonion	5.00	4.50	12.00	11.50	17.50	17.50
20	Supra M^2	12.00	12.00	19.25	19.50	23.75	25.00
21	Occlusal Line	11.00	12.00	17.00	18.25	20.25	23.50
22	Sub M^2	9.50	10.00	15.50	16.00	18.75	19.75

Archer (1997) presents Rhine, Stanley . *Tissue thickness measures: American caucasoids, american blacks, southwestern indians*. Physical Anthropology Labratories,Maxwell Museum of Anthropology, University of New Mexico, 1982,1983, 1984.

Table B2. Tissue depth means (mm) for American Black adults of different weights.

		Emaciated		Normal		Obese	
		Female (N = 5)	Male (N = 4)	Female (N = 10)	Male (N = 27)	Female (N = 2)	Male (N = 1)
	Point Numbers & Descriptions	Mean	Mean	Mean	Mean	Mean	Mean
1	Supraglabella	5.00	4.00	4.50	5.00	3.50	5.00
2	Glabella	6.00	5.25	6.00	6.25	6.00	7.50
3	Nasion	5.25	5.25	5.25	6.00	4.75	5.25
4	End of Nasals	3.25	3.00	3.75	3.75	3.00	3.25
5	Mid Philtrum	10.00	11.75	11.25	12.25	12.00	11.75
6	Upper Lip Margin	12.00	12.50	12.50	14.25	15.25	12.50
7	Lower Lip Margin	12.25	13.75	15.00	15.50	12.00	15.50
8	Chin-Lip Fold	9.50	11.75	12.25	11.75	12.25	13.00
9	Mental Eminence	11.00	11.25	12.50	11.50	13.00	15.25
10	Beneath Chin	6.50	8.00	8.00	8.25	8.50	9.50
11	Frontal Eminence	3.25	3.75	4.00	5.00	5.00	5.50
12	Supraorbital	7.25	7.75	8.00	8.50	8.50	11.75
13	Suborbital	6.50	5.75	8.25	7.75	9.00	9.25
14	Inferior Malar	14.50	14.00	16.75	16.50	18.75	17.50
15	Lateral Orbit	12.00	10.50	13.00	13.25	12.75	20.00
16	Zygomatic Arch, midway	8.00	6.75	9.50	8.25	9.25	13.75
18	Supraglenoid	9.75	9.50	11.50	11.00	17.25	17.50
19	Gonion	11.00	11.50	13.50	13.00	17.50	24.00
20	Supra M^2	20.50	19.00	20.25	22.00	23.50	24.00
21	Occlusal Line	17.75	16.75	19.25	19.00	20.00	30.00
22	Sub M^2	14.25	13.50	17.00	16.50	20.00	23.50

Archer (1997) presents Rhine, Stanley . *Tissue thickness measures: American caucasoids, american blacks, southwestern indians*. Physical Anthropology Labratories,Maxwell Museum of Anthropology, University of New Mexico, 1982,1983, 1984.

Appendix C – Tissue Measurement by Manheim

Table C1. Tissue depth means (mm) for Black adults of normal weight.

		19–34 Years						35–45 Years						45–55 Years		
		Female (*N = 18*)			Male (*N = 19*)			Female (*N = 21*)			Male (*N = 3*)			Female (*N = 5*)		
	Point Numbers & Descriptions	Mean	SD	Range	Mean	SD	Range	Mean	SD	Range	Mean	SD	Range	Mean	SD	Range
1	Glabella	4.6	0.70	4–6	5.2	1.12	3–7	4.5	0.93	3–7	5.3	1.53	4–7	4.8	0.84	4–6
2	Nasion	6.0	0.91	4–8	6.6	0.84	5–8	5.2	1.25	4–8	5.7	2.08	4–8	6.0	1.00	5–7
3	End of nasals	1.7	0.46	1–2	2.2	0.42	2–3	1.5	0.51	1–2	1.7	0.58	1–2	2.0	0.71	1–3
4	Lateral nostril	8.4	1.98	6–12	9.2	2.82	6–15	8.4	2.01	5–13	10.3	2.52	8–13	8.4	1.52	6–10
5	Mid-philtrum	9.2	1.82	6–13	13.0	2.20	10–18	8.8	1.92	6–13	11.0	1.73	9–12	8.2	2.49	6–12
6	Chin lip fold	11.8	2.20	7–15	12.7	2.05	10–17	11.7	2.42	8–18	12.7	1.15	12–14	10.0	2.55	6–13
7	Mental eminence	10.8	2.68	5–15	12.1	2.90	7–18	11.2	2.25	7–15	12.3	4.51	8–17	10.8	3.11	8–16
8	Beneath chin	6.7	2.02	3–10	8.8	1.89	6–13	6.4	2.65	3–12	7.0	2.00	5–9	7.2	1.92	4–9
9	Supraorbital	6.1	0.83	5–7	6.4	1.30	4–9	6.0	1.22	3–9	6.3	0.58	6–7	5.8	0.84	5–7
10	Suborbital	6.2	1.17	5–9	5.8	1.26	3–8	6.9	1.96	4–13	7.0	1.00	6–8	5.8	1.30	5–8
11	Supracanine	10.0	2.28	6–15	12.8	1.86	10–16	9.6	2.75	6–15	10.3	1.53	9–12	9.0	2.45	7–13
12	Subcanine	10.9	2.44	6–15	14.4	2.89	9–21	11.5	1.60	9–15	10.7	0.58	10–11	12.4	3.91	7–17
13	Posterior maxilla	26.6	4.36	18–34	28.2	3.46	23–38	26.8	4.47	19–38	27.3	4.51	23–32	26.8	4.09	22–31
14	Superior mid mandible	21.7	3.99	13–29	24.5	4.05	17–33	22.5	3.93	15–31	23.7	4.04	20–28	21.2	5.89	11–26
15	Inferior mid mandible	12.6	2.85	8–19	14.1	4.21	8–23	13.1	4.17	6–22	13.3	2.31	12–16	13.4	4.04	9–19
16	Lateral eye orbit	5.0	0.84	4–7	4.8	0.76	4–7	4.9	1.18	3–7	3.7	0.58	3–4	4.8	0.84	4–6
17	Anterior zygoma	10.2	2.28	6–15	8.4	2.22	5–13	9.8	2.38	5–15	6.3	0.58	6–7	9.8	3.27	6–15
18	Gonion	17.0	4.23	9–27	21.1	3.24	17–29	16.2	3.64	11–24	20.7	2.89	19–24	14.8	2.86	11–18
19	Root of zygoma	6.4	2.25	3–11	7.4	1.77	5–12	5.6	2.22	3–10	5.7	1.15	5–7	6.0	2.24	5–10

Manhein MH, Listi GA, Barsley RE, Musselman R, Barrow NE, Ubelaker DH. *In vivo facial tissue depth measurements for children and adults.* Journal of Forensic Sciences 2000;45

Table C2. Tissue depth means (mm) for White adults of normal weight.

		19–34 Years						35–45 Years						46–55 Years					
		Female (*N = 52)*			Male (*N = 28)*			Female (*N = 15)*			Male (*N = 10)*			Female (*N =6)*			Male (*N = 5)*		
	Point Numbers & Descriptions	Mean	SD	Range	Mean	SD	Range	Mean	SD	Range	Mean	SD	Range	Mean	SD	Range	Mean	SD	Range
1	Glabella	4.8	0.95	3–7	5.0	0.67	4–6	4.7	1.03	4–7	5.5	1.27	4–7	4.8	1.17	4–7	6.0	1.41	4–8
2	Nasion	5.5	1.16	3–8	6.0	1.12	4–9	5.3	1.39	3–8	6.4	1.43	4–8	6.2	0.75	5–7	7.2	1.64	5–9
3	End of nasals	1.8	0.63	1–4	1.9	0.45	1–3	1.6	0.51	1–2	2.4	0.97	1–4	1.8	0.41	1–2	1.8	0.45	1–2
4	Lateral nostril	8.6	1.99	4–13	7.51	1.9	5–12	8.0	1.73	6–12	9.8	1.81	7–12	10.8	1.94	9–14	10.4	2.51	8–14
5	Mid-philtrum	9.1	1.69	6–13	1.91	2.24	7–17	7.4	1.30	5–10	10.6	1.43	9–13	8.0	1.41	6–10	8.0†	3.00	5–11
6	Chin lip fold	10.3	1.55	6–13	1.1*	1.85	7–15	9.6	1.50	7–12	13.1	1.52	10–15	9.81	2.32	6–12	11.6	1.67	10–14
7	Mental eminence	9.2	2.08	4–14	10.0	2.77	6–17	9.2	2.14	6–14	12.0	3.20	6–17	0.7	2.80	8–15	11.0	1.73	10–14
8	Beneath chin	6.0	1.45	3–9	7.2*	1.73	5–13	5.4	1.84	2–9	8.0	1.05	7–10	6.7	2.94	4–12	7.2	1.79	5–9
9	Supraorbital	5.7	1.04	4–10	5.3	1.25	3–7	5.5	1.19	3–8	5.9	0.88	4–7	6.5	0.84	6–8	7.7	1.67	5–9
10	Suborbital	6.1	1.05	4–8	5.8	1.58	4–11	5.7	1.33	4–9	6.2	1.87	4–11	7.3	4.08	3–15	6.8	0.84	6–8
11	Supracanine	9.3	1.74	5–14	11.9*	2.65	7–17	7.8	1.37	5–10	10.1	2.13	7–13	7.7	1.86	6–10	10.0†	2.00	8–12
12	Subcanine	9.4	1.56	5–12	11.5	2.17	7–16	8.7	2.23	4–12	10.2	1.32	9–13	9.0	2.97	6–12	10.0	2.35	8–14
13	Posterior maxilla	26.3	4.94	11–44	28.5	4.69	21–39	25.1	6.74	13–40	24.6	6.45	12–32	27.2	6.11	20–35	28.2	7.53	17–35
14	Sup mid mandible	23.4	4.53	9–31	25.1	4.15	18–35	20.1	5.15	10–29	21.1	6.69	12–34	21.7	5.32	18–32	21.4	3.85	17–26
15	Inf mid mandible	13.7	3.25	7–22	14.8	4.48	8–25	12.6	4.21	6–22	15.6	4.81	9–23	13.0	4.29	6–17	15.4	4.39	9–20
16	Lateral eye orbit	4.7	0.88	3–8	4.2	0.79	3–6	4.3	0.90	3–6	4.3	0.82	3–5	4.5	1.87	2–7	5.4	0.55	5–6
17	Anterior zygoma	9.3	1.70	6–12	7.8	2.38	4–12	8.7	2.74	4–16	8.2	2.20	4–12	10.2	1.60	9–13	8.2	2.05	5–10
18	Gonion	17.4	3.70	7–27	20.0	4.27	10–31	15.3	4.50	9–25	19.6	5.87	13–30	14.7	4.68	7–20	19.0	4.69	15–25
19	Root of zygoma	7.4	2.07	4–13	7.8	2.29	4–14	4.9	1.44	3–9	6.6	3.86	3–13	6.0	1.55	4–8	5.4	1.52	3–7

* Indicates N = 27 (number excludes men with beards and mustaches).

† Indicates N = 3 (number excludes men with beards and mustaches).

Manhein MH, Listi GA, Barsley RE, Musselman R, Barrow NE, Ubelaker DH. *In vivo facial tissue depth measurements for children and adults.* Journal of Forensic Sciences 2000;45

Appendix D – Tissue Measurement by Helmer

Table D1. Tissue depth means (mm) for White European adults

Point Numbers & Descriptions	20 – 29 years				30 – 39 years				40 – 49 years			
	Female	(N = 12)	Male	(N = 13)	Female	(N = 13)	Male	(N = 14)	Female	(N = 11)	Male	(N = 13)
	Mean	Range	Mean	Range	Mean	Range	Mean	Range	Mean	Range	Mean	Range
1 Vertex	4.5	2.7 – 6.7	5	4 – 6.5	5	4.5 - 5.7	5	4 - 6	5	4 - 5.5	5	3.5 - 7.5
2 TriChion	4.1	3.5 - 5	4.3	3.5 – 5.5	4	3.5 - 5	4.7	3.3 - 6	3.9	3.3 - 5.2	4.5	3.5 - 5.7
3 Metopion	4.5	3.5 - 5.2	5	4 – 5.5	4.5	4 - 5.7	5	3.7 - 6.5	4.6	3.5 - 5.2	5	3.2 - 6.5
4 Ophryon	5	4.2 - 5.8	5.5	5 – 6 – 7	5.2	4.5 - 5.8	5.8	4.5 - 7.5	5.3	3.8 - 6	5.5	3.8 - 7
5 Glabella	5.5	4.5 - 6.3	5.7	5.2 - 6.7	5.7	5 - 6.5	6.2	5 - 7.7	5.9	4.5 - 6.7	6	4.3 - 7.5
6 Nasion	6.9	4.7 - 7.3	8.2	6.3 - 10.2	6.5	6 - 77	7.3	6 - 11.3	6.2	5.3 - 7.5	6.8	5.3 - 8.3
7 Nasal bone	2.9	1.7 - 4.0	3	1.5 - 4.5	3	1.5 - 4.5	3.5	2 - 4.2	3	1.5 - 4.5	3.9	2.5 - 4.5
8 End of nasal	2.3	1.5 – 4.2	2.3	1 - 3.7	2.5	1 - 3.8	2.5	1.5 - 4.0	2.4	1 - 3.2	2.7	1.8 - 4.5
9 Lateral nasal	7	4.8 - 8.5	7,5	5.8 - 9	6.3	4.7 - 8	7.4	5.2 - 9.5	6.7	4.5 - 9.8	7.3	6 - 9.5
10 Alare	11.6	9.3 - 13	13.3	11.2 - 14.5	11	9.2 - 13.7	11.7	10 - 16.2	11	9.2 - 12.3	12.2	9.3 - 14.7
11 Subnasale	13.6	11.5 - 15	15.5	12.3 - 17.2	12.8	11.5 - 14.5	14.6	12.5 - 18.7	12.6	11.5 - 14.5	15.6	9.5 - 19
12 Upper Lip	11.8	10.2 - 14.2	14	11.8 - 17	10.7	9 - 12.8	12.3	9.5 - 17.3	10.5	8.7 - 11.7	12.6	9 - 18.2
13 Lower Lip	12	10.8 - 15.7	14.2	10.5 - 16	12	10 - 13.7	14.9	12.3 - 17.2	12.5	9.5 - 14	14.2	11.5 - 19.2
14 Labionmental	10.4	9.3 - 12.5	12	10 - 14	10.8	8.8 - 12.7	12.1	1.7 - 14.3	12.3	9.5 - 14.2	13.3	10 - 15.8
15 Pogonion	9.6	6.7 - 11.3	9.7	7.3 – 13.7	10	7.3 - 12.2	10.3	7.8 - 13	9.6	5.5 - 11.8	11.7	8.3 - 18.2
16 Gnathion	7.1	5.6 - 8.7	7.5	6.5 - 10	7.2	5.3 - 8.8	8.3	6 - 9.7	6.9	5 - 11	9.5	6.5 - 13.7
17 Lateral foreherad	5.2	4.5 - 5.7	5.5	4.5 - 6.7	5	4.5 - 5.7	6	5 - 7	5.3	4 - 6.3	5.5	4.2 - 7.3
18 Med - Supraorbital	6.6	5.7 - 8	7.3	6.3 - 9.2	6.5	5.8 - 7.5	7.3	6.0 - 8.5	7.4	5.3 - 8.3	7.2	5.3 - 11.7
19 Orbitale	5.5	2.7 - 6.7	5.2	4.2 - 5.7	5.5	3.7 - 8.5	5	4.2 - 8.2	5.4	3.8 - 7.3	5.8	3.3 - 7.5
20 Canine fossa	18.8	15.7 - 21	18.8	16 - 23.7	20.2	16 - 27.7	19.7	16.3 - 24.7	19.1	15 - 23.3	21.5	18.2 - 25.7
21 Upper 1st Molar	19.2	15.8 - 11.7	20.2	15.7 - 25.3	21.5	10 - 29.3	22	16 - 29	20.5	16.8 - 24	21.7	17.8 - 28.7
22 Lower 1st Molar	16.6	13.8 - 20.8	19	14.5 - 24.3	19	14.8 - 29	18.5	15.3 - 23	18	15 - 22.8	18.3	16 - 24.3
23 Mandibular	9.2	6 - 11.5	9.2	6.2 - 11.8	9	5.3 - 13	10.1	5.2 - 15	9.1	7.5 - 12.5	10.2	6.3 - 14.8
24 Frontotempolare	5	4.3 - 5.5	5	4.3 - 6.0	5	4.3 - 8.7	5.3	4 - 6.7	4.8	3.5 - 6.5	5.5	3.8 - 7
25 Lateral orbit	5.2	4.2 - 6	5.3	4.3 - 5.7	5	4.3 - 5	5.2	4.3 - 6.2	5.1	3.5 - 7.5	5.8	5 - 7
26 Lateral zygomatic	8.9	7.5 - 9.8	7.5	6.2 - 9	9	7.2 - 10.7	7.6	6 - 9.5	9.1	6.5 - 11.3	6.8	4.8 - 9.3
27 Zygomaxillar	10.3	8.8 - 12.3	9.5	8.3 - 10.7	10.3	8.3 - 12.8	9.9	5.5 - 12	10.6	7.8 - 14.3	10.1	7.5 - 12.2
28 Midmandible	10.7	8.0 - 13	12	10.7 - 14.3	11.5	9.7 - 15.7	11.9	6.5 - 16.7	11.8	6.8 - 16.7	12.8	8 - 19
29 Euryon	5	4.5 - 7	6	5 - 9.5	5.5	4 - 67	6.7	5 - 9	5	4.5 - 6.5	6.5	44.5 - 8
30 Temporalis	14.2	12 - 17	15.3	13.2 - 18	14.2	8.7 - 19.8	16.3	13.7 - 19.3	14.3	11 - 16.2	16.1	13 - 19.3
31 Zygomatic arch	4.8	4.3 - 5.8	5.3	3.5 - 6.3	5.2	4 - 8.5	5.3	4 - 9.7	5.4	4.3 - 7.8	5.5	4.3 - 8
32 Midmasseter	17.2	13.8 - 21	19.2	15 - 23.3	18.3	14.8 - 22.3	21.3	15.5 - 23	17.8	15.3 - 22.2	20.4	13.7 - 29.8
33 Gonion	11.6	9.2 - 16	11	6.3 - 15.8	11.7	9.7 - 16.2	13.2	8.5 - 16.3	11.2	9.5 - 14.5	13.3	3.5 - 1.8
34 Opisthocranium	4.5	4 – 6	5.5	4.5 - 6.5	5	3.5 - 5.5	5.5	4.5 - 6.5	5	3.5 - 6.5	5.5	4.5 - 7.5

Wilkinson (2004), modified from Helmer, R (1984). *Schädelidentifizierung durch elektronische Bildmischung*. Heidelberg, Kriminalistik-Verlag

Table D2. Tissue depth means (mm) for White European adults

Point Numbers & Descriptions	50 – 59 years				60+ years			
	Female	(N = 15)	Male	(N = 11)	Female	(N = 11)	Male	(N = 10)
	Mean	Range	Mean	Range	Mean	Range	Mean	Range
1 Vertex	5	4 - 7	5	4 - 65	5	3.5 - 6.3	4.8	3.5 - 6.7
2 TriChion	4	3 - 4.7	4.7	3.7 - 6.3	4	3.7 - 5.5	4.9	3.8 - 5.8
3 Metopion	4.7	3.5 - 5.2	5	4 - 6	5.2	4.2 - 5.5	4.8	4 - 6
4 Ophryon	5.3	3.8 - 6.3	5.8	5 - 6.5	5.8	5 - 7.2	5.8	4.5 - 7.3
5 Glabella	6	4.5 - 7	6	5.5 - 7	6.5	5.3 - 7.3	6.3	5 - 7.7
6 Nasion	6.5	4.8 - 7.5	7.3	6.2 - 8.2	6.5	5.5 - 7.7	7.1	6 - 9.2
7 Nasal bone	3	1.5 - 4	3.5	1.5 - 6.3	3	2.2 - 3.8	3.7	2.8 - 5
8 End of nasal	2.3	1.5 - 4.3	2.8	1 - 4	2.5	1.8 - 3.5	2.6	1.3 - 4.3
9 Lateral nasal	6.5	5.5 - 9.7	8.2	6.3 - 12.8	7.3	5 - 10.2	6.7	5.7 - 10
10 Alare	11.5	10 - 12.8	12.5	10.8 - 13.7	11.5	9.5 - 12.8	11.9	9.7 - 14.3
11 Subnasale	13.2	10 - 15.7	14.3	12.2 - 19.5	12.2	9.7 - 14.2	12.9	8.5 – 15.3
12 Upper Lip	10	8.2 - 14.5	11.8	9.3 - 14.8	9.8	8.7 - 10.3	9.9	7.7 - 11.7
13 Lower Lip	11.8	9.8 - 16.2	13	11.5 - 16.8	11.5	9.7 - 15.3	12.7	11.5 - 16
14 Labionmental	12.2	10.2 - 13.2	13	12 - 16.3	12.7	10.3 - 15.3	12.8	11.2 - 15.3
15 Pogonion	11.3	8 - 13.5	13.7	9.7 - 17.3	12	8.8 - 13.8	12.3	10.3 - 14.7
16 Gnathion	8	5.5 - 11.3	9.8	7 - 12.7	8.7	6 - 12.2	8.9	8 - 11.7
17 Lateral foreherad	5	4 - 6.3	6	4.5 - 8	5.3	4.5 - 6.5	6.2	4.8 - 7.5
18 Med - Supraorbital	6.7	6 - 7.5	7.5	6.2 - 8.5	6.8	6.3 - 8	6.7	5.8 - 8.2
19 Orbitale	6	3.5 - 8	5.5	4.7 - 9.7	6.3	5.2 - 10.7	5.8	3.7 - 11.7
20 Canine fossa	20.7	14.7 - 24.7	21.8	17 - 24.5	22.3	18.2 - 28	21.5	15.7 - 24
21 Upper 1st Molar	19.3	14.3 - 23.3	22.3	14 – 28.3	20.5	11.8 – 26.3	18.8	13.8 - 23.2
22 Lower 1st Molar	17.7	15 - 21.7	18.3	16.3 - 21.8	19	11.3 - 24	17.2	14.7 - 19.8
23 Mandibular	9	5.3 - 11.3	12	8.8 - 15.7	10.3	8 - 13.7	10.3	9.5 - 12.5
24 Frontotempolare	5	3.5 - 6.3	5.5	4 - 7.8	5	4 - 5.3	5.5	4 - 6.7
25 Lateral orbit	5.3	4 - 5.8	5.7	4.8 - 7	5.5	4.5 - 7.2	5.6	4.2 - 6.7
26 Lateral zygomatic	9	6.2 - 10.8	8	6.3 - 12	10.3	6.7 - 13	7.5	5.3 - 9.5
27 Zygomaxillar	10.7	6.5 - 12.7	10.7	9.2 - 13.2	12.2	7.5 - 15	9	6.5 - 11.2
28 Midmandible	12.2	9.8 - 15.5	14.2	11.8 - 20 - 5	13.7	11.3 - 19.3	13.4	11.2 - 16.3
29 Euryon	5.3	4 – 7.2	7	5.5 - 8	5.2	4.5 - 6	6.4	5.3 - 7.8
30 Temporalis	13.3	4.3 - 19.2	14.7	14.3 - 22.3	13.3	11.3 - 18.5	14.9	8.7 - 17.2
31 Zygomatic arch	5.3	4.3 - 7	5.5	4.8 - 10.8	5.2	4.5 - 10	5	3.8 - 8.2
32 Midmasseter	17.3	13.7 - 22	20.5	17.7 - 23	19.2	15.8 - 23.7	20.6	16.3 - 25.3
33 Gonion	10.3	4.3 - 14.5	11.7	6.7 - 17.7	14.3	11.2 - 17.3	14.4	7.5 - 17.3
34 Opisthocranium	5	4 - 7	5.5	4.5 - 7.5	5	3.5 - 6.3	5.5	4.5 - 7.7

Wilkinson (2004), modified from Helmer, R (1984). *Schädelidentifizierung durch elektronische Bildmischung*. Heidelberg, Kriminalistik-Verlag

Appendix E – GUI

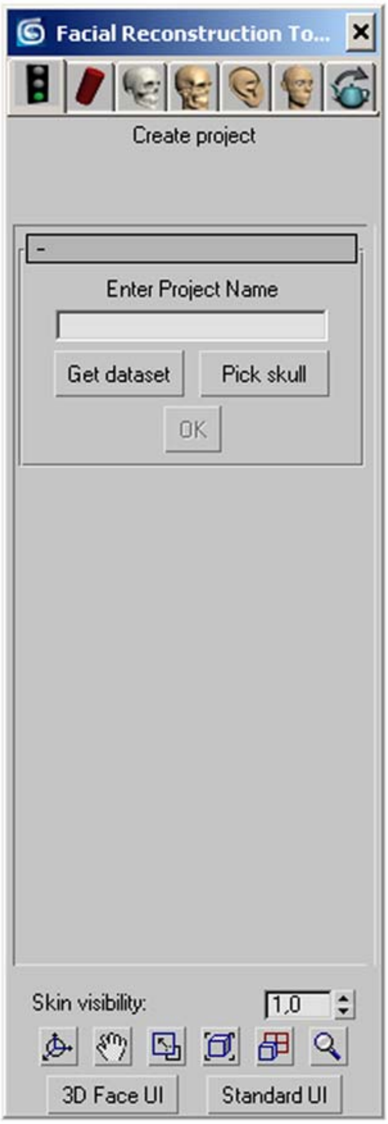

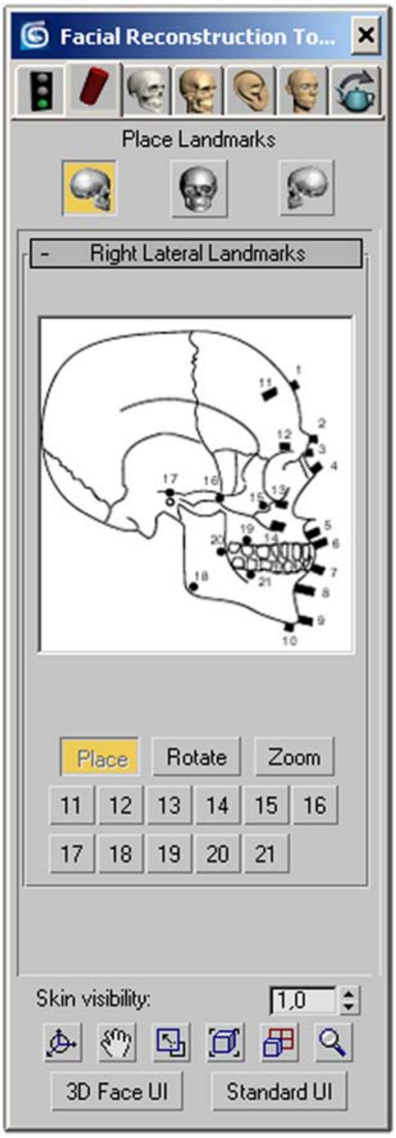

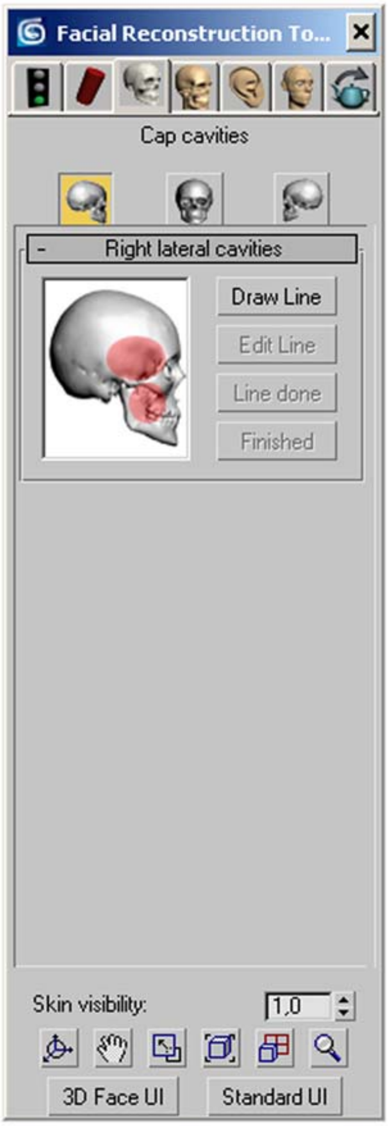
Facial Reconstruction To...
Cap cavities
Right lateral cavities
Draw Line
Edit Line
Line done
Finished
Skin visibility:
1,0
3D Face UI
Standard UI


Facial Reconstruction To...
Create skin
Create the skin
Load tissue depth data
Default dataset loaded
Create skin
Skin visibility:
1,0
3D Face UI
Standard UI


Facial Reconstruction To...
Create facial features
Create eyes
Select right
Select left
End selection
Redo selection
Reposition eye centers
Right eye
Left eye
Eye width
Eye height
Skin visibility:
1,0
3D Face UI
Standard UI

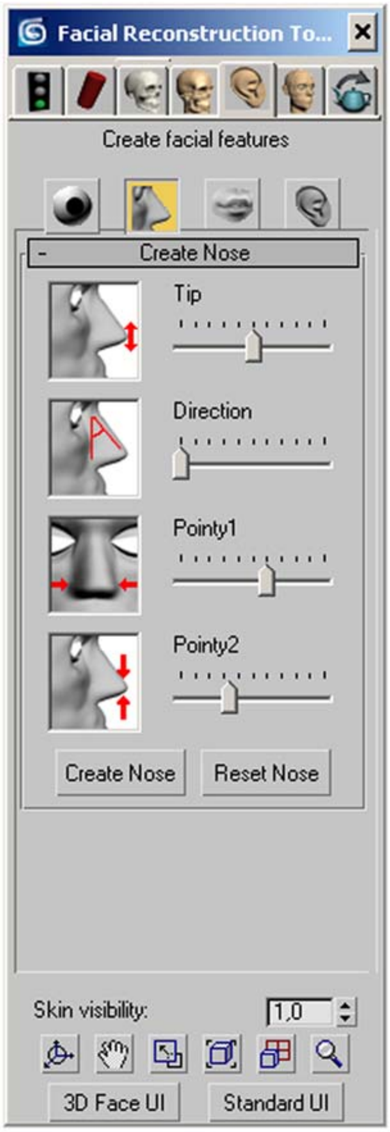
Facial Reconstruction To...
Create facial features
Create Nose
Tip
Direction
Pointy1
Pointy2
Create Nose
Reset Nose
Skin visibility:
1,0
3D Face UI
Standard UI

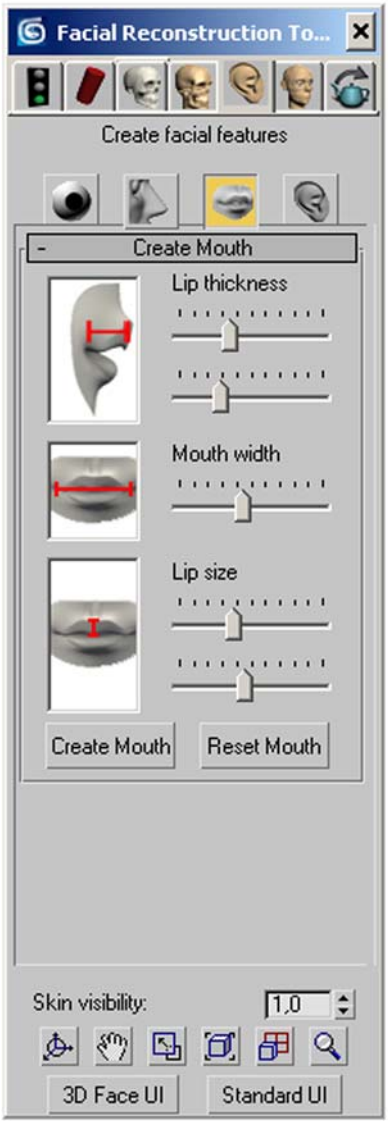
Facial Reconstruction To...
Create facial features
Create Mouth
Lip thickness
Mouth width
Lip size
Create Mouth
Reset Mouth
Skin visibility:
1,0
3D Face UI
Standard UI


Facial Reconstruction To...
Create facial features
earMaker
Ear Size
Ear Rotation
Ear Tilt
Create Ears
Reset Ears
Skin visibility:
1,0
3D Face UI
Standard UI


Facial Reconstruction To...
Edit skin
- Post-processing
Push/Pull Values: 5,0
Brush Size 10,0
Brush Strength: 1,0
Push/Pull
Relax
Skin visibility: 1,0
3D Face UI
Standard UI

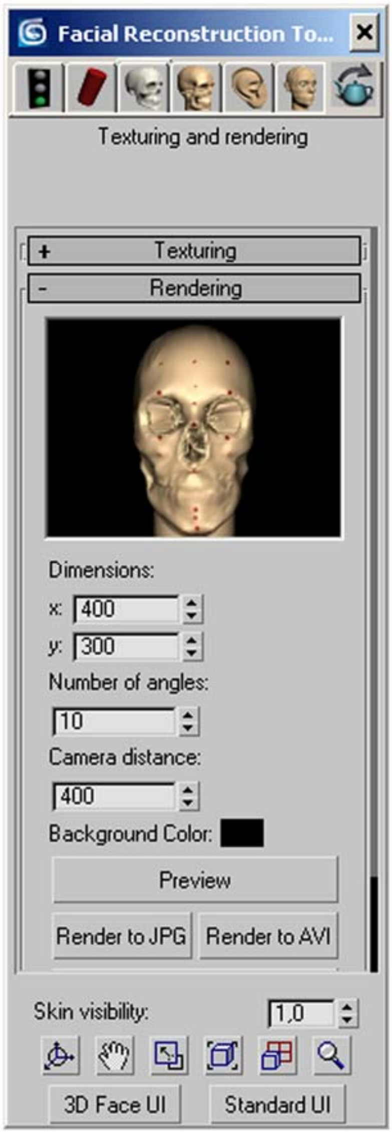
Facial Reconstruction To...
Texturing and rendering
+ Texturing
- Rendering
Dimensions:
x: 400
y: 300
Number of angles:
10
Camera distance:
400
Background Color:
Preview
Render to JPG
Render to AVI
Skin visibility: 1,0
3D Face UI
Standard UI